Lund University

FYSK02

Measurement & Feedback Control of a Two-Level System

Author: Sayan Nikolai Ali Khan
Supervisor: Peter Samuelsson & Björn Annby-Andersson
Thesis submitted for the degree of Bachelor of Science
July 5, 2022

LUND UNIVERSITY

Project duration: 2 months (15 ECTS)
Examination Date: May 2022
Department of Physics, Division of Mathematical Physics

Contents

Abstract

In this bachelor project, the main objective is to investigate how a two-level quantum system can be controlled using weak continuous measurements and feedback control. The Monte-Carlo method was used to simulate the system dynamics under measurement and feedback to investigate how the system state can be controlled. This thesis concludes on how the feedback function impacts the purity of the state, represented by the Bloch vector on a Bloch sphere. The applications of this project extend to quantum information.

Popular Science Abstract

How may one measure a highly sensitive system without disturbing it? This bachelor's project will investigate the possible techniques of measuring and controlling a quantum two-level system.

A two-level quantum system may be likened to a nightclub, where there are people that like all genres of music. Essentially, if a certain jam is being played, the people who enjoy that song will go on the dancefloor and start throwing shapes. Analogously, the particles in a quantized system will be excited by an external stimulus, which allows the particles to move from a calm state to an excited state. To be able to observe the particles moving around, one needs to introduce a measurement technique, which must be sensitive enough to be able to extract little information but not strong enough to affect the system. A quantum system reacts to any external impulse much like climate and weather can be affected by the concentration of greenhouse gases in the atmosphere. Therefore, it is incredibly important that one understands how the quantum system may be affected through the measurement process. In this project, the focus will lie on implementing an existing measurement technique which can be applied to continuously evolving systems through "poking" at the system repeatedly. Unfortunately, theory suggests that repeated poking of the system may still lead to an undesirable effect onto the quantum system. This undesirable quantum effect is known as the Quantum Zeno effect and is often referred to as a measurement paradox. The mining of information from a quantum system may result in mixed results, in other words, one may obtain a mixture of two states, which leads to complications with respect to the interpretations.

Why are quantum technologies, specifically measurement instruments, so crucial in the upcoming future? Many technological gadgets are using so-called lithium-ion technology to store and provide electrical power. Unfortunately, the abundance of lithium salts is diminishing much like it has for oil for the past decades. Considering the latest news on the shortage of semiconductor technology, inventions and innovations are indispensable to curb the carbon emissions due to anthropological processes in an energy hungry society. The complexity revolved around the energy network in modern society provides major incentives for technological developments and societal adaptations. It should not appear as a surprise that many countries have invested a considerable amount of money on developing quantum technologies to minimize the energy consumption. On a political level, discussions have been held about carbon dioxide emissions such as the Paris Climate Accords COP 2015. As an example the history of automobiles, where a vast majority of the technology has shifted from analogue to digital based systems has shown an increase propulsion efficiency inducing a reduction in carbon emissions.

The feedback control aspect of the project relates to how one can inject energy into the system to obtain a desired state. A more popular system that features a feedback control system is known as a PID system utilized in electric vehicles. A specific example is featured in electric vehicles, where the car detects a stop signal and the controller sends a signal to the DC motor engine to gradually break [1]. Similarly, in this project the secondary objective

is to create a similar control and feedback system, which implies that one can inject energy into the two-level system in the hopes of controlling the outcome. Regarding the nature of a two-level system, one must consider probabilistic models which can simulate all possible outcomes with specified parameters. The probabilistic model, called Monte Carlo method, has its origins from the simulation of several blackjack tables at a Monte Carlo Casino and has gained its significance through its effectiveness to simulate kinetic models of gas [2].

Feedback and Control Systems are of major relevance to modern technology. A famous example that hosts feedback protocols are robots that have ultrasound sensors. The feedback and control system acts as an ad hoc to a measurement of any given system. An additional example of an implemented control and feedback system are electric vehicles. Featuring self-driving capabilities as well as regenerative breaking capacities are systems that exist in many electric vehicles. These concepts may be likened to the two-level quantum system, where one may consider the injection of energy as the control part and the POVM measurement as the measurement and feedback. Similarly, many modern cars feature a so-called traction control system, which helps the driver re-centre the car in case of driving on slippery roads by giving the wheels different amount of torques. The combination of a brain-like system on an existing mechanism can improve the efficiency of a system. Furthermore, with access to artificial intelligence, the computer models can advise on design improvements, reducing the necessary energy. Measurements has been a central aspect of physical systems for multiple decades as it represents one of the most crucial elements of the natural sciences, namely empirical studies.

The results of the simulation will enlighten us on better understanding how to apply quantum mechanics in modern technology for more efficient energy usage. As a secondary consequence, one may gain a better understanding of how quantum mechanical systems behave under a nano-scope.

Acknowledgement

I would like to extend my deepest gratitude to some impeccable people that I have met so far on my journey called life. First and foremost, Carl Johan Bérard Varnauskas and Nadine Hassan, you have helped me through some of the toughest days here in Sweden ever since I started my bachelors degree in 2018. The days and evenings that we have spent together are among the brightest in my life thus far. Gustavo Abraham Garcia Alvarez, even though I only know you for a couple of months, it is not due to the lengthiness of time spent together that I cherish the dear moments, but it is the intensity of our exchange. I am deeply grateful to be quantum entangled as a friend with you. Our discussions on how physics impacts our daily lives is a delight and you allow me to widen my spectrum of knowledge. Muchas gracias amigo! Darejan Tsurtsumia, the Georgian, you have helped me through some of my toughest emotional moments ever and I honour and appreciate that with all my heart. Carlos Daniel Camona, the jokes that you have told me have made me laugh so hard and I thank you dearly for your support and good vibes. Fredrik Granström and Annie Csomor, my fellow physicist friends, if I had not met you I do not think I would have developed the skills and intuition I have today. I am looking forward to the future discussions that we may share in the future. I thank you both for supporting me when I was struggling with the courses. I would also like to extend my deepest gratitude and heart warming acknowledgement to all the other people I have met in my life so far, if it was not for the encounter I may have not had the chance to reflect and grow as a person intellectually, emotionally and spiritually.

Maneeza, Rita & Osman, Mom & Dad, my beloved family, it has been an extremely tough journey since I was born on 16th december 1993. Had I not had any of your love and support I do not think I would be who I am today nor would I have achieved as much as I have so far. Merci beaucoup, je vous aime.

Professor Peter Samuelsson & Björn Annby-Andersson, Morten, Faraj, Saulo, Daniel, Drilon, and all other members of the research group. If there is one phrase that I could say to express my gratitude and learnings from joining the group discussions and working on the project it would be "I feel that thanks to you all I am more quantum mechanically informed about the complexity of nature, even though I know I have only scratched the surface." Emmanuel D Costa, I know we only met recently but it has been a grand pleasure to study alongside you as well as listening to your advice on learning physics.

I fundamentally believe that light traverses all dimensions of the space-time continuum, that is why when life gets tough one shall strive to see the silver lining in the given moment. Perseverance is what makes us who we are, only with determination and discipline can one attain their goals. Here are a couple of quotes that have followed me since my childhood. Chi va piano, va sano e lontano. As one of my idols has said, Richard Philipps Feynman, "Physics is not the most important thing in life. Love is." Another quote that inspired me is by none other than Commander Spock. "Live long and prosper."

List of Acronym

- POVM: Positive Operator Valued Measure

My Contributions

The simulation and calculations were carried out in a self-written Python script using the Spyder IDE with the assistance and guidance of the supervisors.

1 Introduction

The topic for my bachelor project concerns *Measurement & Feedback Control of a Two-Level System*. As is suggested in the title, there are two main parts to the thesis. The first part concerns the different possible types of measurements and how one can obtain information from a two-level quantum system. The second part mainly concerns how to apply so-called feedback protocols to control the system based on the measurement outcome. The main objective of this project is to assess and understand how one could develop quantum measurement techniques and feedback control protocols for quantum technologies.

The most common measurement type is known as the von Neumann measurement. The measurement technique is based on a projection of the system onto one of the eigenstates of the measured observable. Given that we project the system onto one of the eigenstates of the observable, this may alter the the system state by doing the measurement. Consequently, the von Neumann measurement has one major trade-off, where more information of a given system may be obtained, but the measurement procedure strongly affects the system state. If such a measurement is repeated several times in infinitely short time steps, the results will be identical every time.

One may go beyond the concept of the *von Neumann measurements*. This is referred to as generalized quantum measurements, and describes any types of measurements, including the *von Neumann* type. As described above, the *von Neumann measurement* describes how the wavefunction of the measured system is collapsed under measuring. This is regarded as a strong interaction. Within the framework of generalized quantum measurements, it is also possible to describe measurements that weakly interacts with the system, preserving the pre-measurement wavefunction. This is central to this thesis, where one wants to continuously measure the state of a quantum two-level system. To this end, it is important tha the measurement is weak such that the state of the system is preserved. A generalized measurement is considered relatively flexible in the sense that it varies in the degree of affecting the system. A strong type of generalized measurement technique, known as projective measurement or von Neumann measurement, as mentioned before yields a "direct" measurement, or a snapshot of the state. The two mentioned measurement techniques consist of different ways of extracting information from a quantum system. In this project, a simulation based on a Monte-Carlo model will be applied. The need for quantum measurement techniques is largely supported by the fact that one would like to be able to control the state. One cannot control a quantum system without slightly disturbing the system.

Some examples that illustrate this concept is the use of quantum bits, which essentially represents a superposition of the two possible states, $|0\rangle$ and $|1\rangle$. The ability to host a superposition of the state is a basis for quantum computers in order to control the computer through quantum logic gates [4]. One seeks the ability to control the state of the quantum bits. The system hosts two quantized states, on $|1\rangle$ and off $|0\rangle$. One may consider the lowest atomic level as the ground state $|0\rangle$ and the next level as the first excited state $|1\rangle$, which can be referred to as a transition between atomic states. In quantum computers, the advantage to host a superposition of states allows for a higher computational power [4].

All in all, considering the two possible measurement techniques introduced, one can deduce why a generalized measurement would be favourable with respect to applied quantum mechanics in future applications. In a nutshell, being able to construct a quantum system that can be measurable and controllable to a certain degree allows for a myriad of advantages. The specific Monte-Carlo simulation model will clarify the different possible outcomes, which parameters affect the system and possibly to what degree. Furthermore, due to the nature of quantum mechanics, technologies can be designed around the mentioned flexibility opening a new realm to the nano-electronics, quantum device technology and quantum information industry. The results indicate that depending on how strong of a measurement strength and interaction strength one sets, the stronger the backaction of the feedback and hence less pure the state will be.

2 Theory

The theory related to quantum measurements and feedback control may be structured into three main topics

- Density Operator,
- Generalized measurement or Positive Operator Valued Measure and
- Time Evolution of Quantum Measurements.

The first section will briefly describe the relevant theory, which gives the framework for a *generalized measurement* or *Positive Operator Valued Measure*, abbreviated *POVM*.

2.1 Density Operator Theory

2.1.1 Definition of Density Operator & Properties

The density operator, denoted $\hat{\rho}$, describes in a generic way the state vector, in other words it represents the observer's state of knowledge of a system [5]. The *ensemble of pure states* of a given system is expressed as follows

$$\hat{\rho} := \sum_{i=1}^{N} p_i \left|\psi_i\right\rangle \left\langle\psi_i\right|, \tag{1}$$

where $p_i \leq 1$ represents the probabilities and the $|\psi_i\rangle$ the states. The associated properties are given below

$$\begin{aligned}
&\hat{\rho}^\dagger = \hat{\rho}, \\
&Tr\{\hat{\rho}\} = 1, \\
&\langle\phi|\hat{\rho}|\phi\rangle = \sum_{i=1}^{N} p_i \langle\phi|\psi_i\rangle \langle\psi_i|\phi\rangle = \sum_{i=1}^{N} p_i |\langle\phi|\psi_i\rangle|^2 \geq 0, \\
&\hat{\rho}(t+\Delta t) = \hat{U}(\Delta t)\hat{\rho}(t)\hat{U}^\dagger(\Delta t),
\end{aligned} \tag{2}$$

where $|\phi\rangle$ is an arbitrary state vector [3]. The first property shows that the *density operator* $\hat{\rho}$ is hermitian, the second property shows that the trace of a density matrix, the sum of the populations, is always equal to 1. The third property is more commonly known as the *positivity condition*. The last property states that the density matrix at time t can be transformed to the density matrix at a later time $t + \Delta t$, for any arbitrary time interval time Δt, by the unitary operator $\hat{U}(\Delta t)$. Additionally, it describes how the *density operator* $\hat{\rho}$ translates with respect to time [3]. Due to the third property, positivity condition, the *density matrix* can be written as

$$\hat{\rho} := \sum_{i=1}^{N} \Lambda_i \left|\alpha_i\right\rangle \left\langle\alpha_i\right| , \tag{3}$$

where Λ_i represents the associated eigenvalues for the respective eigenstates $|\alpha_i\rangle$ of the density matrix [3].

For a closed system, the density operator is subjected to a *unitary transformation* $U(t)\hat{\rho}(t)U^{\dagger}(t)$ with respect to time t, given by Eq.(2). An additional crucial property is the time differentiation of the *density operator* $\hat{\rho}$. On that note, one may express the so-called *Schrödinger-von Neumann equation*, given by

$$\partial_t \hat{\rho} = -\frac{i}{\hbar}[\hat{H}, \hat{\rho}]. \tag{4}$$

Given the aforementioned equations and properties one may describe in detail the density matrix. When the system state is pure, one of the probabilities in Eq.(1) is equal to 1, with the other probabilities being 0, and the density matrix is given by [5]

$$\hat{\rho} := \left|\Psi\right\rangle \left\langle\Psi\right| . \tag{5}$$

The *physical content* of the *density operator* $\hat{\rho}$ may be represented by the matrix representation with respect to an orthonormal basis, which is represented by the basis states $|\beta\rangle$. The *density matrix elements* are given by [5]

$$\rho_{\beta\beta'} := \left\langle\beta|\hat{\rho}|\beta'\right\rangle . \tag{6}$$

The elements on the matrix's diagonal are known as the *populations*, which yield the probability of being in the chosen state $|\beta\rangle$ [5]

$$\rho_{\beta\beta} = \left\langle\beta|\hat{\rho}|\beta\right\rangle = |\left\langle\beta|\psi\right\rangle|^2. \tag{7}$$

The off-diagonal elements are known as *coherences*. The coherences between the *pure states* may be expressed as a phase shift [5]

$$\rho_{\beta\beta'} = |c_\beta c_{\beta'}| \cdot \exp\{[i(\phi_\beta - \phi_{\beta'})]\}. \tag{8}$$

A *pure state* is described as having a particle in a particular state $|\psi_i\rangle \langle\psi_i|$, hence it can be described by the definition Eq.(5), whereas one may more generally describe the density operator $\hat{\rho}$ for *mixed states* as follows [3] (c.f. Eq.(1)). Conclusively, knowing the existence of pure states and generic mixed states, one can conclude the following two properties [5]

$$\begin{aligned} \text{Pure State}: \ & |\rho_{\beta\beta'}|^2 = \rho_{\beta\beta} \cdot \rho_{\beta'\beta'}, \\ \text{Mixed State}: \ & |\rho_{\beta\beta'}|^2 < \rho_{\beta\beta} \cdot \rho_{\beta'\beta'}, \ \beta \neq \beta'. \end{aligned} \tag{9}$$

A further discussion may be held about the contrast between *pure state* and *mixed state* described by Eq.(9). As prescribed by *normalization*, one may make the following conclusions [5]

$$\text{Pure State}: \; Tr\{\hat{\rho}^2\} = Tr\{|\psi\rangle \langle\psi|\psi\rangle \langle\psi|\} = Tr\{\hat{\rho}\} = 1, \tag{10}$$

where $Tr\{\hat{\rho}^2\}$ is known as *purity*, implying that for *pure states* the following strictly holds $Tr\{\hat{\rho}^2\} = 1$. When the density matrix can be written as $\hat{\rho} = \frac{1}{N}$ in an arbitrary orthonormal basis, where N describes the dimension of the system, we refer to the system as being *maximally mixed*. For such states, we obtain the purity

$$Tr\{\hat{\rho}^2\} = \frac{1}{N}. \tag{11}$$

2.1.2 Expectation Value

In this subsection, we show how the density operator can be used to calculate the expectation value of an arbitrary operator $\hat{A}$. For a pure state $|\psi\rangle$, the expectation value is given by [5]

$$\left\langle \hat{A} \right\rangle := \langle\psi|\hat{A}|\psi\rangle \, . \tag{12}$$

Especially, note that this can be written as

$$Tr\{\hat{A}\} := \sum_i \langle\alpha_i|\hat{A}|\alpha_i\rangle \, . \tag{13}$$

For a mixed state, we thus get

$$\left\langle \hat{A} \right\rangle = \sum_j p_j \langle\psi_j|\hat{A}|\psi_j\rangle = Tr\{\hat{A}\hat{\rho}\}. \tag{14}$$

2.1.3 Bloch Sphere

The *Bloch sphere* is a unit spherical geometrical representation of the states of a given two-level quantum system. As an example the *Fig.* (1) below illustrates for a two-level quantum system. The *Bloch sphere* is introduced in the field of *quantum computation* and *quantum information*, which yields a visualization of the *state* of a *single qubit*.

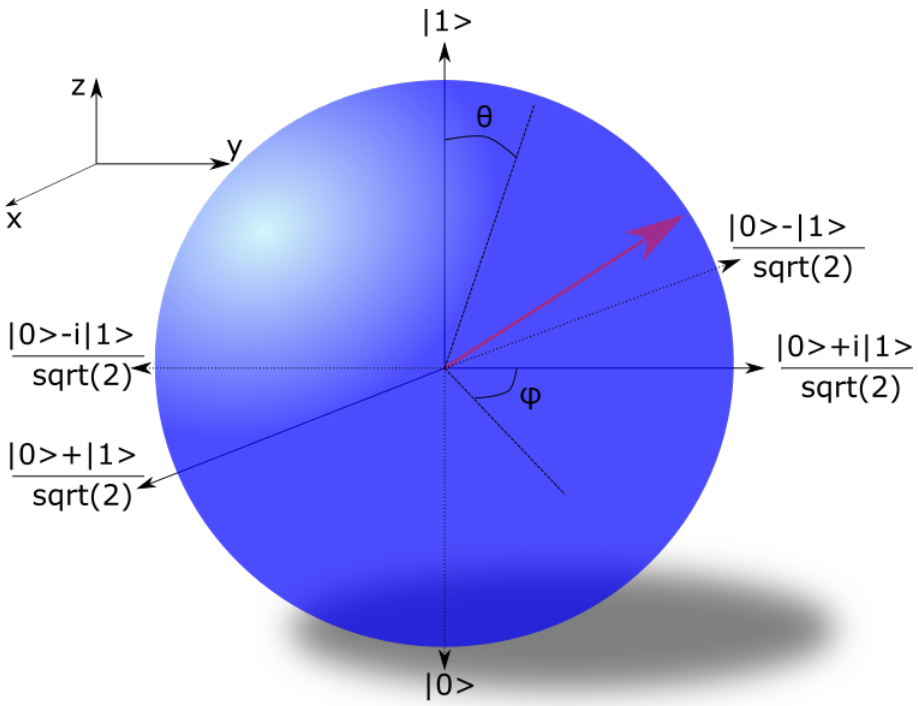

Figure 1: An example of a Bloch Sphere for a Two-level system.

The red vector, known as the Bloch vector in *Fig.* (1) has a variable magnitude, which represents the purity of the state. If the vector is of unit length, then the state is *pure*. It's azimuthal φ and polar angle θ are indicative of the probability of obtaining one of the states with respect to a three-dimensional Cartesian coordinate system $\{x, y, z\}$, whose positive and negative axes represent the states in the *Fig.* (1). A superposition of states on the *Bloch sphere* is given by [3]

$$|\psi\rangle = e^{i\gamma}\left[\cos\left(\frac{\theta}{2}\right)|0\rangle + e^{i\varphi}\sin\left(\frac{\theta}{2}\right)|1\rangle\right]. \tag{15}$$

Given the spherical representation *Eq.* (15) above, one may mathematically express the different possible states in a system through a *density matrix*. The *density operator* $\hat{\rho}$ may be represented by the *Bloch vector* $\vec{r}$ as [3]

$$\hat{\rho} = \frac{\mathbb{I} + \vec{r}\cdot\sigma}{2}, \ \|\vec{r}\| \leq 1, \tag{16}$$

where $\sigma = (\sigma_x, \sigma_y, \sigma_z)$ represents the *Pauli spin matrices*. The *Pauli spin matrices* are defined as follows [3]

$$\sigma_x = \begin{pmatrix} 0 & 1 \\ 1 & 0 \end{pmatrix}, \ \sigma_y = \begin{pmatrix} 0 & -i \\ i & 0 \end{pmatrix}, \ \sigma_z = \begin{pmatrix} 1 & 0 \\ 0 & -1 \end{pmatrix}, \tag{17}$$

which are written on the $|0\rangle$ and $|1\rangle$ basis. The respective components of the *Bloch vector* $\vec{r} = r_x\hat{x} + r_y\hat{y} + r_z\hat{z}$ can be obtained through the trace

$$r_j = Tr\{\hat{\sigma}_j\hat{\rho}\}. \tag{18}$$

2.2 Quantum Measurements

2.2.1 Generalized Quantum Measurements and Positive Operator Valued Measure (POVM)

A generalized quantum measurement or positive operator valued measure (POVM) is based on the following postulate [3]:

Definition 1. *Measurement Postulate*
"Quantum measurements are given by a collection $\{\hat{\Omega}_m\}$ *of measurement operators. These are operators acting on the state space of the system being measured. The index* m *refers to the measurement outcomes that may occur in the experiment. If the state of the quantum system is* $|\psi\rangle$ *immediately before the measurement the probability that the result* m *occurs is described by* $p(m) = \langle\psi|\hat{\Omega}_m^\dagger\hat{\Omega}_m|\psi\rangle$*."*

A quantum measurement may be exercised under the presumption that a collection of *measurement operators* $\{\hat{\Omega}_m\}$ is defined. Consequentially, one may express the outcome of a probability $p(m)$, under the pretext that the quantum system at hand is described by the density operator $\hat{\rho}$ [3], hence

$$p(m) = Tr\{\hat{\Omega}_m^\dagger\hat{\Omega}_m\hat{\rho}\}. \tag{19}$$

The state of the system after a measurement may be expressed in conjunction with *Eq.*(19) [3]

$$\hat{\rho'} = \frac{\hat{\Omega}_m\hat{\rho}\hat{\Omega}_m^\dagger}{p(m)}. \tag{20}$$

The *measurement operators* $\{\hat{\Omega}_m\}$ must satisfy the following *completeness relations* [3]

$$\begin{aligned} &\sum_m \hat{\Omega}_m^\dagger\hat{\Omega}_m = \mathbb{I}, \\ &\sum_{m=1}^{N} Tr\{\hat{\Omega}_m^\dagger\hat{\Omega}_m\hat{\rho}\} = 1. \end{aligned} \tag{21}$$

A major dilemma concerned with quantum measurements is that a measurement on any quantum particle, implies that the carried information will be erased or destroyed and consequently the state of the particle will be altered. The most common type of quantum measurements is the von Neumann, or projective measurement. This type of measurement describes how the measured system is projected onto one of the eigenstates of the measured observables, and completely erases the pre-measurement state. To avoid such a projection, one can perform a weak measurement, which only weakly interacts with the system and preserves the pre-measurement state. In this section, we begin by introducing the properties of a generalized measurement, and then study the von Neumann measurement, and lastly the special case of the generalized measurement, known as the *measurement operator* $\hat{K}(z)$. After, introducing the framework related to generalized measurements and POVM, a discussion on continuous measurement is explored.

The two measurements, *strong projective* and *weak*, which will be detailed subsequently are supported by the postulate (1) [3]. Furthermore, the *state* of the system after the measurement is given by

$$\frac{\hat{\Omega}_m |\psi\rangle}{\sqrt{\langle\psi|\hat{\Omega}_m^\dagger \hat{\Omega}_m|\psi\rangle}}. \tag{22}$$

Using the *postulate* 1 above, one may define a *strong projective measurement*. A common type of measurement operator is known as the *projective measurement* is described by a *hermitian* operator on the *state space* of a chosen state being observed. An arbitrary measurement operator $\hat{A}_m$ needs not to be a projection. The *post-measurement state* does not yield us any additional information about the probabilities of the respective *measurement outcomes* $p(m)$, as described by *Eq.*(19). In order to perform a so-called **positive-operator valued measure** POVM, one may define a *positive operator*. A positive operator may be defined as follows [3]

$$E_m := \hat{\Omega}_m^\dagger \hat{\Omega}_m. \tag{23}$$

The *completeness relation Eq.*(21) and the *probability* $p(m)$ of the outcome m is given by

$$p(m) = \langle\psi|\hat{E}_m|\psi\rangle\,. \tag{24}$$

The previously aforementioned equations show that the set of operators $\{\hat{E}_m\}$ are collectively known as a POVM. In *quantum computation* and *quantum information* to be able to have a decent amount of control on a state of a given system, one performs a *general measurement*. A type of general measurement is introduced subsequently.

The most common form of measurement taught in courses of *quantum mechanics* is based on *projection*. The *projection* implies that the system will collapse onto one of the possible *eigenstates* of a given measured *observable* $\hat{A}$. The *eigenstates* $|\alpha_i\rangle$ $i = \{1, \cdots, N\}$, where the *probability* of finding the system in state $|\alpha_i\rangle$ is given by the Born rule [5, 6],

$$p(i) = |c_i|^2 = |\langle\alpha_i|\psi\rangle|^2. \tag{25}$$

The *von Neumann measurements*, represent a specific type of measurements, which can be described by the projection operator $\hat{\mathcal{P}}$ [5]. The *measurement operator* $\hat{A}$ is constructed with the use of the *projection operator* $\hat{\mathcal{P}}$ [3]

$$\hat{\mathcal{P}}_i := |\alpha_i\rangle\langle\alpha_i|\,,\ i \in \{1, \cdots, N\}. \tag{26}$$

Consequently, a *spectral decomposition* can be constructed

$$\hat{A} = \sum_m m \cdot \hat{\mathcal{P}}_m. \tag{27}$$

The *von Neumann measurement*, based on the projection operator $\hat{\mathcal{P}}_i$, projects the system onto an eigenstate, and we know with certainty the post-measurement state. Consider the

initial state of a given system to be described by the *density operator* *Eq.*(1). If we obtain as a result $|\alpha_i\rangle$, the post-measurement state is [5]

$$\hat{\rho}_f = |\alpha_i\rangle \langle\alpha_i| = \frac{\hat{\mathcal{P}}_i \hat{\rho} \hat{\mathcal{P}}_i}{Tr\{\hat{\mathcal{P}}_i \hat{\rho} \hat{\mathcal{P}}_i\}}. \tag{28}$$

The trace in the denominator gives the probability of obtaining an outcome $|i\rangle$ and yields the same as *Eq.*(25). This *probability* can also be calculated with the following equation

$$p(i) = Tr\{\hat{\mathcal{P}}_i \hat{\rho} \hat{\mathcal{P}}_i\} = |c_i|^2. \tag{29}$$

Note that the projection operators satisfy the completeness relation

$$\sum_{i=1}^{N} \hat{\mathcal{P}}_i^\dagger \hat{\mathcal{P}}_i = I, \tag{30}$$

and the following property

$$\hat{\mathcal{P}}_i \hat{\mathcal{P}}_j = \delta_{ij} \hat{\mathcal{P}}_i. \tag{31}$$

The aforementioned quantities may be given by [5]

$$\begin{aligned} \hat{\rho}_f &= \frac{\hat{\Omega}_m \hat{\rho} \hat{\Omega}_m^\dagger}{Tr\{\hat{\Omega}_m \hat{\rho} \hat{\Omega}_m^\dagger\}}, \\ p(m) &= Tr\{\hat{\Omega}_m \hat{\rho} \hat{\Omega}_m^\dagger\}. \end{aligned} \tag{32}$$

A *weak measurement* is often associated with a weak interaction with the system at hand. Given an operator $\hat{A}$, consider the special case, where one defines the measurement operator $\hat{K}(z)$ given by

$$\hat{K}(z) := \left(\frac{2\lambda\delta t}{\pi}\right)^{1/4} \cdot e^{-\lambda \cdot \delta t \cdot (z - \hat{A})^2}. \tag{33}$$

A *weak* quantum measurement is commonly described as a type of *POVM measurement*. As described by equation *Eq.*(19), one may use the properties of the density operator $\hat{\rho}$ to associate with a measurement operator $\hat{K}(z)$. Consequently, the measurement operator $\hat{K}(z)$ inherits the properties given by *Eq.*(21) and *Eq.*(22). One chooses to define the measurement of *operators* to be given as a *weighted sum* of *projectors* onto the *eigenstates* $|\alpha_i\rangle$ of $\hat{A}$; the operator may be defined as follows [5]

$$\hat{K}(z) := \left(\frac{2\lambda \cdot \delta t}{\pi}\right)^{1/4} \sum_{i=1}^{N} \exp\Big\{[-\lambda \cdot \delta t \cdot (z - \hat{A})^2]\Big\} \cdot |\alpha_i\rangle \langle\alpha_i|. \tag{34}$$

One may, based on *Eq.*(34), have either [5]

- a *weak measurement* $\lambda \ll 1$, which preserves *quantum coherences*, the *off-diagonal* terms or
- a *strong measurement* $\lambda \gg 1$, which represents a projective measurement.

2.2.2 Measurement Operator & Property

Consider the *measurement operator* $\hat{K}(z)$ *Eq.*(33), one can verify that applying the *hermitian conjugate* times the operator $\hat{K}^\dagger(z) \cdot \hat{K}(z)$ yields the identity operator $\mathbb{I}$. Hence, one wants to show that the following holds

$$\int_{-\infty}^{\infty} \hat{K}^\dagger(z)\hat{K}(z)dz = \mathbb{I}. \tag{35}$$

One can verify that this completeness relation *Eq.* (30) holds for a two-level system, where the Pauli-Z operator

$$\hat{\sigma}_z = -\left|0\right\rangle\left\langle 0\right| + \left|1\right\rangle\left\langle 1\right|. \tag{36}$$

Consequently, this corresponds to measuring whether the ground state $|0\rangle$ or the first excited state $|1\rangle$ is occupied. By plugging *Eq.* (33) and the Pauli-Z operator $\hat{\sigma}_z$ into the left-hand side of *Eq.* (35), one obtains

$$\int_{-\infty}^{\infty} \left(\frac{2\lambda\delta t}{\pi}\right)^{1/2} e^{-\lambda\delta t(z-\hat{\sigma}_z)^{2\dagger}} \cdot (\left|0\right\rangle\left\langle 0\right| + \left|1\right\rangle\left\langle 1\right|) \cdot e^{-\lambda\delta t(z-\hat{\sigma}_z)^2} \cdot (\left|0\right\rangle\left\langle 0\right| + \left|1\right\rangle\left\langle 1\right|)dz = \mathbb{I}, \tag{37}$$

which verifies that the completeness relation holds.

2.2.3 Density Operator & Measurement Operator Behaviour

The *density operator* for an arbitrary set of operators $\Omega = \{\hat{M}_1, \hat{M}_2, \cdots, \hat{M}_N\}$ is defined as in *Eq.*(32). In a two-level system, one may define the *density operator* as

$$\hat{\rho} = P_0\left|0\right\rangle\left\langle 0\right| + \alpha(\left|0\right\rangle\left\langle 1\right| + \left|1\right\rangle\left\langle 0\right|) + P_1\left|1\right\rangle\left\langle 1\right|, \ \alpha \in \mathbb{R},$$
$$\hat{\rho} = \begin{pmatrix} P_0 & \alpha \\ \alpha & P_1 \end{pmatrix}.$$

Given the previous density $\hat{\rho}$, one would like to assess how the *measurement operator* $\hat{K}(z)$ acts in the limits

- $\lambda \to \infty$: von Neumann projection,
- $\lambda \to 0$.

Consider a function $\hat{f}(z) := \hat{K}(z)\hat{\rho}\hat{K}^\dagger(z)$, the function may be decomposed in the following sense

$$\begin{aligned}\hat{f}(z) = \sqrt{\frac{2\lambda\delta t}{\pi}} \cdot \Bigg[& P_0 \cdot e^{-\lambda\delta t(\hat{z}-\hat{\sigma}_z)^2}\left|0\right\rangle\left\langle 0\right| e^{-\lambda\delta t(\hat{z}-\hat{\sigma}_z)^{2\dagger}} + \alpha e^{-\lambda\delta t(\hat{z}-\hat{\sigma}_z)^2}\left|0\right\rangle\left\langle 1\right| e^{-\lambda\delta t(\hat{z}-\hat{\sigma}_z)^{2\dagger}}, \\ & + \alpha e^{-\lambda\delta t(\hat{z}-\hat{\sigma}_z)^2}\left|1\right\rangle\left\langle 0\right| e^{-\lambda\delta t(\hat{z}-\hat{\sigma}_z)^{2\dagger}} + P_1 e^{-\lambda\delta t(\hat{z}-\hat{\sigma}_z)^2}\left|1\right\rangle\left\langle 1\right| e^{-\lambda\delta t(\hat{z}-\hat{\sigma}_z)^{2\dagger}} \Bigg], \\ \lambda \to 0 \implies & \hat{f}(z) = 0.\end{aligned} \tag{38}$$

The result obtained expresses that no information has been extracted from taking a measurement with strength $\lambda \to 0$. If one takes the following integral, applying the *Gaussian integral*, for the case $\lambda \to \infty$

$$\begin{aligned}\int_{-\infty}^{\infty} \hat{f}(z)dz &= \sqrt{\frac{2\lambda\delta t}{\pi}} \cdot \int_{-\infty}^{\infty} \left[P_0 \cdot e^{-2\lambda\delta t(\hat{z}+1)^2} \left|0\right\rangle \left\langle 0\right| + P_1 e^{-2\lambda\delta t(\hat{z}-1)^2} \left|1\right\rangle \left\langle 1\right| \right] dz, \\ &= P_0 \cdot \delta(z+1) \left|0\right\rangle \left\langle 0\right| + P_1 \cdot \delta(z-1) \left|1\right\rangle \left\langle 1\right|.\end{aligned}$$

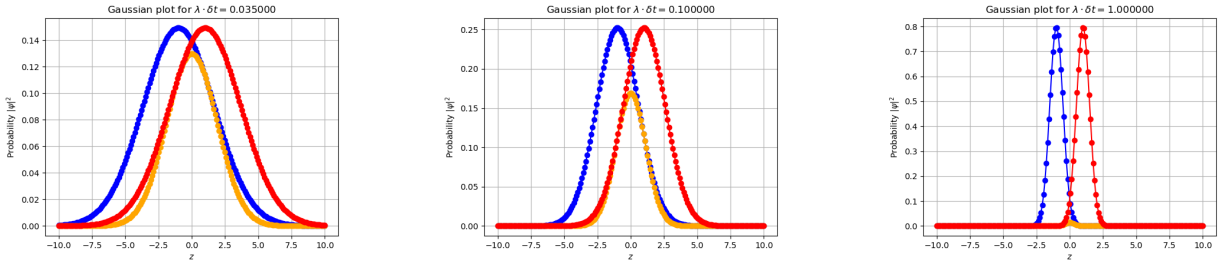

(a) $\bar{\lambda} = \lambda \cdot \delta t \to 0.035$ (b) $\bar{\lambda} = \lambda \cdot \delta t \to 0.1$ (c) $\bar{\lambda} = \lambda \cdot \delta t \to 1.0$

Figure 2: *Figures* (2a), (2b), (2c) showing the Gaussian distribution for for a two-level system in the respective cases. In the first case, the off-diagonal terms, or mixed state terms, survive for a very small λ. In the last case, that in *Fig.* (2c), when the measurement strength λ is high, the yellow peak vanishes completely, which implies no off-diagonal terms.

2.2.4 Continuous Measurements

Continuous measurements are indispensable in order to evaluate the state of a system. The advantage of a continuous measurement is that one can know the state of the system at all times, which is paramount for the control of quantum bits in a quantum computer. One may consider with respect to the density operator $\hat{\rho}(t)$, the continuous measurement equation

$$\hat{\rho}_t(z_1, \cdots, z_n) = \cdots e^{-i\hat{H}\delta t} \hat{K}(z_1) \hat{\rho}_{t0} \hat{K}^\dagger(z_1) \cdot e^{i\hat{H}\delta t} \cdots, \tag{39}$$

where each measurement z_i is taken at an infinitesimal small time step $\delta t \to 0$ with respect to a given *Hamiltonian* $\hat{H}$, to simulate a continuous measurement. In the limit $\delta t \to 0$, one obtains a continuous measurement.

2.3 Time Evolution Under Continuous Measurements

One may equally look at how continuous measurements affect the quantum system. A consequence of the back action of a weak continuous measurement, the time evolution of the system will be affected. An effect that occurs during incremental time measurements is commonly known as the *Quantum Zeno effect*.

2.3.1 Time Evolution of Continuous Measurements

Consider a time-dependent *density operator* $\hat{\rho}_t$, which is defined by *Eq.*(39). The *Hamiltonian* $\hat{H}$ of the *two-level system* is given as follows

$$\hat{H} = \epsilon \left|1\right\rangle \left\langle 1\right| + g \cdot \left(\left|0\right\rangle \left\langle 1\right| + \left|1\right\rangle \left\langle 0\right|\right) + 0 \left|0\right\rangle \left\langle 0\right|. \tag{40}$$

Given this information, one may determine the time-derivative of the time-dependent *density operator* $\dot{\hat{\rho}}(t)$ based on *Eq.*(39) for a two-level system, where $\hat{\sigma}_z$ is getting measured and $\hbar = 1$ [9], hence

$$\frac{d\hat{\rho}(t)}{dt} = -\frac{i}{\hbar}\Big[\hat{H}, \hat{\rho}\Big] + \lambda \cdot \Big(\hat{\sigma}_z \hat{\rho} \hat{\sigma}_z - \hat{\rho}\Big). \tag{41}$$

2.3.2 Rabi Oscillator

In this first case, we seek to evaluate the behaviour of the system when

- $\epsilon = 0$,
- $\lambda = 0$,

in *Eq.*(41), which is more commonly known as the *Rabi Oscillator*, where $\hbar = 1$. Given the differential *Eq.*(41), one may express the time-derivative of the *density operator* $\dot{\hat{\rho}}(t)$, hence

$$\begin{aligned}
\frac{d\hat{\rho}}{dt} &= -i \cdot \Big[g\Big(\left|0\right\rangle \left\langle 1\right| + \left|1\right\rangle \left\langle 0\right|\Big), \hat{\rho}\Big] + 0 \\
&= -i \cdot \Big[g\Big(\left|0\right\rangle \left\langle 1\right| + \left|1\right\rangle \left\langle 0\right|\Big) \cdot \Big(P_0(t) \left|0\right\rangle \left\langle 0\right| + \alpha(t) \left|0\right\rangle \left\langle 1\right| + \alpha^*(t) \left|1\right\rangle \left\langle 0\right| + P_1(t) \left|1\right\rangle \left\langle 1\right|\Big) \\
&\quad - \Big(P_0(t) \left|0\right\rangle \left\langle 0\right| + \alpha(t) \left|0\right\rangle \left\langle 1\right| + \alpha^*(t) \left|1\right\rangle \left\langle 0\right| + P_1(t) \left|1\right\rangle \left\langle 1\right|\Big) \cdot g\Big(\left|0\right\rangle \left\langle 1\right| + \left|1\right\rangle \left\langle 0\right|\Big)\Big]
\end{aligned}$$

Consequently, one obtains four differential equations, where one may express the differential *Eq.*(41) as follows

$$\frac{d\hat{\rho}}{dt} = \dot{P}_0(t) \left|0\right\rangle \left\langle 0\right| + \dot{\alpha}(t) \left|0\right\rangle \left\langle 1\right| + \dot{\alpha}^*(t) \left|1\right\rangle \left\langle 0\right| + \dot{P}_1(t) \left|1\right\rangle \left\langle 1\right|. \tag{42}$$

By matching the terms from the above *density operator* time-derivative *Eq.*(42) with the result obtained from the other formulation of the time-derivative *Eq.*(41), one obtains

$$\begin{aligned}
\dot{P}_0(t) &= -ig\Big(\alpha^*(t) - \alpha(t)\Big), \\
\dot{P}_1(t) &= -ig\Big(\alpha(t) - \alpha^*(t)\Big), \\
\dot{\alpha}(t) &= -ig\Big(P_1(t) - P_0(t)\Big), \\
\dot{\alpha}^*(t) &= -ig\Big(P_0(t) - P_1(t)\Big).
\end{aligned}$$

Knowing that we have the following conditions, where the initial condition, denoted by $\hat{\rho}_0$, represents the $|0\rangle$ state to be occupied, one may make the following deductions

$$\begin{aligned}
\hat{H} &= g\Big(|0\rangle\langle 1| + |1\rangle\langle 0| \Big) = g\hat{\sigma}_x, \\
\hat{H} &= g\begin{pmatrix} 0 & 1 \\ 1 & 0 \end{pmatrix}, \\
\hat{\rho}_{t_0} &= \sum_j p_j \, |\psi_j(t_0)\rangle \langle \psi_j(t_0)| \, , \\
\hat{\rho}_t &= e^{-i\hat{H}(t-t_0)} \hat{\rho}_{t_0} e^{i\hat{H}(t-t_0)} \\
t_0 = 0: \;\; \hat{\rho}_0 &= \begin{pmatrix} 1 & 0 \\ 0 & 0 \end{pmatrix}, \\
e^{-i\theta\hat{\sigma}_x/2} &= \begin{pmatrix} \cos(\theta/2) & -i\sin(\theta/2) \\ -i\sin(\theta/2) & \cos(\theta/2) \end{pmatrix}.
\end{aligned}$$

The last matrix describes a *Givens rotation* about the $x-$ axis in a 2-D plane with the multiplication of the *Pauli Spin-X matrix* multiplied by the complex number i. The result yields

$$\begin{aligned}
\hat{\rho}_t &= \begin{pmatrix} \cos(gt) & -i\sin(gt) \\ -i\sin(gt) & \cos(gt) \end{pmatrix} \cdot \begin{pmatrix} 1 & 0 \\ 0 & 0 \end{pmatrix} \cdot \begin{pmatrix} \cos(gt) & i\sin(gt) \\ i\sin(gt) & \cos(gt) \end{pmatrix} \\
&= \begin{pmatrix} \cos^2(gt) & i\frac{1}{2}\sin(2gt) \\ -i\frac{1}{2}\sin(2gt) & \sin^2(gt) \end{pmatrix}.
\end{aligned} \tag{43}$$

If one were to take the trace of the matrix $\hat{\rho}_t$, it would end up in states being represented by the **diagonal** terms, also known as *populations*, as described in *Eq.*(1) $p_i = 1$ for a at least one state, where as the **off-diagonal** terms, known as *coherent superpositions* of the states $|0\rangle$ and $|1\rangle$, represent the *pure state* given by *Eq.*(1) $p_j \neq p_{j+1} \neq 0$. The solution obtained above *Eq.*(43) is a common problem treated in *Sakurai* [6], where one considers a time-dependent two-state problem, which leads to the formulation of the *Rabi formula* and the associated probabilities [6]. Considering the degenerate case, where $\omega = 0$ and $\omega \approx \omega_{12}$, one obtains the same result as given above, where $g = \frac{\gamma}{\hbar}$ (c.f. 5.1). This particular case is known as the *Rabi resonance condition* [6].

2.3.3 Effect on Measurement

Consider the case, where the time dependent *density operator* $\hat{\rho}(t)$, as according to *Eq.*(41), has the following conditions

- $g = 0$,
- $\epsilon = 0$,

where $\epsilon = 0$ translates to the neglect of the time evolution, in order to evaluate the effect of the continuous measurement. The *Hamiltonian* of the considered two-level system is given by

$$\hat{H} = 0,$$

hence the differential *Eq.*(41) becomes

$$\frac{d\hat{\rho}}{dt} = \lambda(\hat{\sigma}_z\hat{\rho}\hat{\sigma}_z - \hat{\rho}).$$

Given the above equation and expressing the relevant quantities in a matrix form, one obtains

$$\lambda \cdot \left(\hat{\sigma}_z\hat{\rho}\hat{\sigma}_z - \hat{\rho}\right) = \lambda \cdot \left(\begin{pmatrix} 1 & 0 \\ 0 & -1 \end{pmatrix} \cdot \begin{pmatrix} P_0(t) & \alpha(t) \\ \alpha^*(t) & P_1(t) \end{pmatrix} \cdot \begin{pmatrix} 1 & 0 \\ 0 & -1 \end{pmatrix} - \begin{pmatrix} P_0(t) & \alpha(t) \\ \alpha^*(t) & P_1(t) \end{pmatrix} \right),$$

$$\lambda \cdot \left(\hat{\sigma}_z\hat{\rho}\hat{\sigma}_z - \hat{\rho}\right) = \lambda \cdot \begin{pmatrix} 0 & -2\alpha(t) \\ -2\alpha^*(t) & 0 \end{pmatrix} = -2\lambda\Big(\alpha(t)\left|0\right\rangle\left\langle 1\right| + \alpha^*(t)\left|1\right\rangle\left\langle 0\right|\Big).$$

The differential equations as prescribed by *Eq.*(42) yields

$$\begin{aligned} &\dot{\alpha}(t) = -2\lambda\alpha(t) \implies \alpha(t) = C \cdot e^{-2\lambda t}, \\ &\dot{\alpha}^*(t) = -2\lambda\alpha^*(t) \implies \alpha^*(t) = C^* \cdot e^{-2\lambda t}, \\ &P_0(t) = A,\ P_1(t) = B,\ A + B = 1. \end{aligned}$$

Consequently, one may express the *density operator* $\hat{\rho}_t$ in this particular case as

$$\begin{aligned} \hat{\rho}_t &= \begin{pmatrix} A & C \cdot e^{-2\lambda t} \\ C^* \cdot e^{-2\lambda t} & B \end{pmatrix}, \\ \lim_{t\to\infty} \hat{\rho}_t &= \begin{pmatrix} A & 0 \\ 0 & B \end{pmatrix}. \end{aligned}$$

As one can see that over time as measurements are taken, a special effect occurs, where only the ground state $\left|0\right\rangle\left\langle 0\right|$ and the first excited state $\left|1\right\rangle\left\langle 1\right|$ remain, which can be explained through the *Quantum Zeno Effect*.

Referring to *Eq.*(41), one may extend it to a *N-state system*. The *N-state system* case is referred to as the *master equation*, *Linbladian* or *quantum Liouvillian*, where the time derivative of the *density operator* $\dot{\hat{\rho}}$ is given through the *Liouvillian super-operator*, denoted as $\mathcal{L}$ [7]. Consider a quantum dynamical system, where one may define the *Liouvillian super-operator* $\mathcal{L}$ as a linear mapping. A possible formulation of the *master equation* is commonly known as *Markovian quantum master equation*, where the operator $\hat{G}$ is defined subsequently [7]

$$\begin{aligned} \mathcal{L}\hat{\rho}(t) &= -i[\hat{H}, \hat{\rho}] + \{\hat{G}, \hat{\rho}\} + \sum_{i,j=1}^{N^2-1} a_{ij}\hat{F}_i^\dagger\hat{\rho}\hat{F}_j, \\ \hat{G} &:= -\frac{1}{2}\sum_{i,j=1}^{N^2-1} a_{ij}\hat{F}_i^\dagger\hat{F}_j. \end{aligned} \tag{44}$$

One may describe the dimension of the associated Hilbert space as $dim\mathcal{H} = N$ [7]. The subsequent properties are relevant in a N multi-particle system

$$\begin{aligned} &\frac{d}{dt}\rho(t) = \mathcal{L}\rho(t), \\ &(\hat{F}_i, \hat{F}_j) := Tr\{\hat{F}_i^\dagger\hat{F}_j\} = \delta_{ij},\ i = \{1, 2, \cdots, N\}, \end{aligned} \tag{45}$$

where $\hat{F}_i, \hat{F}_j$, represent **orthonormal operators** in a complex space of dimension N^2 *Eq.*(45).

2.3.4 Quantum Zeno Effect

One may describe the **quantum zeno effect** or **quantum zeno paradox** as a consequence of continuously measuring the system "forcing"/collapsing the system into a possible state [8].

Cook proposed an experiment to test the effect on a trapped, cooled ion, in other words deprived of thermal excitation, where a perturbation was applied upon the given system with *resonance frequency* $\omega_{21} = \frac{\Delta E}{\hbar} = \frac{(E_2 - E_1)}{\hbar}$ [8]. Since, spontaneous decay may occur it is very difficult to observe the effect. The probability of a state decaying over a short time δt after a collapse grows quadratically [8]. This applied to a two-level system, where one attributes a probability to the respective state yields [8]

$$\begin{aligned} P_0(t) + P_1(t) &= 1, \\ P_0(t) &= \cos^2(\Omega\tau/2), \\ P_1(t) &= \sin^2(\Omega\tau/2), \end{aligned} \tag{46}$$

where Ω represents the *Rabi frequency*. One generally conducts measurements after a short time such that $\Omega \cdot \tau \ll 1$, most certainly leading to a collapse of the system on the initial state.

3 Method

3.1 Monte-Carlo Method: Density Population Evolution

In this bachelor project, the positive operator measurements, denoted by $\hat{K}(z)$ *Eq.*(33), previously described, were executed as a simulation, where the underlying approach relies on the so-called *Monte-Carlo method*. The *Monte-Carlo method* was applied to simulate several trajectories of the evolution of the density operator $\hat{\rho}$. Finally, we averaged over all trajectories to determine the general behaviour of the system.

3.2 Simulation of the Density Population Evolution

The time-dependent density operator $\hat{\rho}(t)$ is based on a rotation matrix, which induces a rotation in the *Bloch's Sphere* (c.f. *Fig.* (1)), denoted as $\mathcal{L}$. The matrix below $\mathcal{L}$ acts on a column vector of the density matrix $\hat{\rho}(t)$, where the initial condition is given as

$$\mathcal{L}(ig) := \begin{pmatrix} 0 & 0 & ig & -ig \\ 0 & 0 & -ig & ig \\ ig & -ig & 0 & 0 \\ -ig & ig & 0 & 0 \end{pmatrix}, \quad \hat{\rho}(t=0) = \begin{pmatrix} P_0 \\ P_1 \\ \alpha \\ \alpha^* \end{pmatrix}, \tag{47}$$

where this matrix representation corresponds to the *Rabi oscillator*, see section 2.3.2. In addition, the position measurement parameter z is dependent on a normal distribution $\mathcal{N}(\mu, \sigma)$ dependent on a randomized variable x, which represents a randomly selected probability.

This randomized probability is obtained through the diagonal elements of the density matrix. From *Eqs.*(32)-(38), we know that the probability of obtaining outcome z is given by

$$P[z(t)] = \frac{1}{\sqrt{2\pi}\sigma} \exp\left\{-\left(\frac{(z(t)-x(t))^2}{2\sigma^2}\right)\right\},\ x(t) = [-1,1],\ \sigma = \sqrt{\frac{1}{4\lambda\cdot\delta t}}. \tag{48}$$

The random variable $x(t)$ represents the state of the two-level system, where -1 corresponds to $|0\rangle$ and $+1$ to $|1\rangle$. The measurement operator $\hat{K}(z)$ is given by the following matrix $\mathcal{M}$, which stems from *Eq.*(38)

$$\mathcal{M}(z(t)) := \sqrt{\frac{2\lambda\cdot\delta t}{\pi}} \begin{pmatrix} e^{-2\lambda\cdot\delta t\cdot(\hat{z}(t)+1)^2} & 0 & 0 & 0 \\ 0 & e^{-2\lambda\cdot\delta t\cdot(\hat{z}(t)-1)^2} & 0 & 0 \\ 0 & 0 & e^{-2\lambda\cdot\delta t\cdot(\hat{z}^2(t)+1)} & \\ 0 & 0 & 0 & e^{-2\lambda\cdot\delta t\cdot(\hat{z}^2(t)+1)} \end{pmatrix}, \tag{49}$$

where the outcome $z(t)$ has a Gaussian distribution. Based on this explanation and the defined matrices $\mathcal{L}$ and $\mathcal{M}$, one may calculate the new state of the density population using a time step $\delta t = 10^{-3}$ s, hence mathematically the density population matrix is is given by

$$\begin{aligned} \hat{\rho}(t+\delta t) &= \underbrace{\begin{pmatrix} \rho(t_0)_{00} & \cdots & \rho(t_N)_{00} \\ \rho(t_0)_{11} & \cdots & \rho(t_N)_{11} \\ \alpha^*(t_0) & \cdots & \alpha^*(t_N) \\ \alpha(t_0) & \cdots & \alpha(t_N) \end{pmatrix}}_{N},\ \hat{\rho}(t_0) = \begin{pmatrix} 1 \\ 0 \\ 0 \\ 0 \end{pmatrix} \\ \hat{\rho}(t+\delta t) &= \frac{\exp\{(\mathcal{L}\cdot\delta t)\}\cdot\mathcal{M}\cdot\hat{\rho}(t)}{Tr\{\mathcal{M}\cdot\hat{\rho}(t)\}}, \end{aligned} \tag{50}$$

each column of the matrix above $\hat{\rho}(t+\delta t)$ is calculated with *Eq.*(50).

This Hamiltonian $\hat{H}$, together with the von Neumann equation *Eq.*(4), yield the time evolution given in *Eq.*(47), where we have vectorized the density matrix and rewritten the von Neumann equation as a matrix equation. Here, we use the convention $\hbar = 1$, such that the *interaction strength* g is given in units of 1/s. The Hamiltonian $\hat{H}$ is given by

$$\hat{H} = 0\,|0\rangle\langle 0| + g\,|0\rangle\langle 1| + g\,|1\rangle\langle 0| + 0\,|1\rangle\langle 1|\,. \tag{51}$$

Given the equation *Eq.*(51), one may build a program which executes the evolution of the *density operator* $\hat{\rho}(t)$ through *Eq.*(50). One must define a parameter g, which represents the *interaction strength* of the transition states between $|0\rangle$ and $|1\rangle$, whereas ϵ represents the energy of the excited state, denoted $|1\rangle\langle 1|$. A feedback protocol was introduced in order to observe how the system would react if energy was fed back into the system. The feedback protocol was conceptualized as a function $D(z)$ in terms of a parameter $\gamma = 1/\tau$. The parameter γ represents the response rate of the detector, given in 1/s. In other words, one could deduce the following

- $\gamma >> 1\ \text{s}^{-1} \implies \tau << 1$ s,

- $\gamma << 1\ \mathrm{s}^{-1} \implies \tau >> 1\ \mathrm{s}$,

where τ represents the time scale of the measuring detector. The response rate of the detector determines how accurate the feedback can be applied. If $1/\gamma$ is much smaller than the *characteristic time scale* of the system $1/g$, the detector can resolve all system transitions and apply the appropriate feedback consistently. When $1/\gamma$ approaches or is larger than the *interaction strength* $1/g$, the delay of the detector results in feedback errors, as the state of the system may change before the feedback is applied. The time step used in the simulation is of the order $\delta t = 10^{-3}$ s. In this particular project, the γ parameter serves as a measure of the delay of the feedback that is desired. The feedback function is defined as given [12]

$$\begin{aligned} D(t) &= \int_{-\infty}^{t} \gamma e^{-\gamma(t-s)} z(s) ds, \\ D(t+\delta t) &:= D(t) + \gamma \cdot \delta t \cdot (z(t) - D(t)). \end{aligned} \tag{52}$$

The feedback function $D(t+\delta t)$ (c.f. *Eq.*(52)) will either rotate the state vector in the *Bloch's sphere* (c.f. *Fig.* (1)) clockwise or anti-clockwise around the $x-$ axis, depending on the sign of the new value $D(t+\delta t)$, hence depending on the sign of $D(t+\delta t)$ a positive $\mathcal{L}$ or a negative $-\mathcal{L}$ was used in *Eq.*(50). The following plots *figures* (3a) and (3b) show how the feedback function $D(z,t)$ and the average measurement outcome $\hat{\sigma}_z$ evolve over time. The *Fig.* (3a) shows the average measurement outcome with a small delay $\gamma = 10.0$ and the *Fig.* (3b) has a slightly larger delay $\gamma = 5.0$.

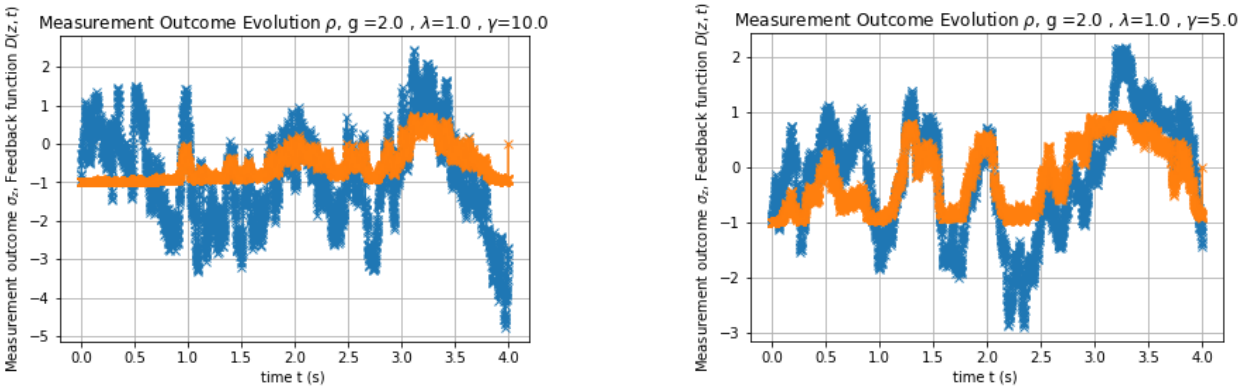

(a) (b)

Figure 3: *Figures* (3a) and (3b) shows how $\hat{\sigma}_z$ and the feedback function $D(t)$ evolve over time for different measurement strengths λ and the delay factor of the feedback γ.The orange curve represents the average measurement outcome $\hat{\sigma}_z$, whereas the blue curve represents the feedback function $D(t)$.

In order to obtain a decent predictive model of the behaviour of the two-level system, several trajectories have been simulated. The trajectories represent different sequences of evolution of the *density operator* $\hat{\rho}(t)$, which vary with respect to the randomized value x given by *Eq.*(48). Subsequently, the values at each time step t_i have been arithmetically averaged to obtain the mean behaviour of the individually coefficients $\rho_{00}, \rho_{11}, \alpha, \alpha^*$.

The *Bloch Sphere*, which was chosen to be projected onto the $yz-$ plane, is described by the following equation, where $|\Psi\rangle$ represents the state vector

$$\vec{r} = i(\alpha^*(t_j) - \alpha(t_j))\hat{e}_y + (\rho_{11}(t_j) - \rho_{00}(t_j))\hat{e}_z,\ j = \{0, \cdots, N\}. \tag{53}$$

As one can read from *Eq.*(53), the *Bloch vector* $\vec{r}$ will vary in angle θ and radius r with respect to time implicitly. An additional test was implemented to verify that the simulation follows what had been hypothesized by the theoretical models described in the theory section 2.2.1. The trace of the matrix as expressed in *Eq.*(9) was calculated to plot the evolution of the *purity trace* $Tr\{\rho^2\}$.

4 Results & Discussion

In the results presented below, the parameters refer to the Hamiltonian given by *Eq.*(51) as well as the feedback function described by *Eq.*(52). Several trajectories, denoted by M were taken to obtain the average evolution $\hat{\bar{\rho}}$. The main objective is to evaluate how the different parameters affect the stationary state of the system. It is especially crucial to investigate whether one can indeed prepare a pure qubit state, despite the presence of dephasing, which is shown by the dampening of the off-diagonal terms, due to the measurement and feedback protocol. The plot of the density matrix elements shows how they are affected by the feedback on the level of a single trajectory. The plot of the density matrix elements averaged over many trajectories illustrates how the density matrix evolves taking many experimental runs into account. The latter is important for understanding common trends in the system dynamics that are not distinguishable on the level of the single trajectories. The Bloch vector gives a geometrical representation of the dynamics of the state. The purity plot illustrates how pure the state actually is. The numerical computation time ranged from 13 mins. 40 s to 19 mins. 56 s dependent on the parameters used.

Measurement Strength $\lambda = 1.0 \cdot 10^{-5}$ and $g = 2.0$

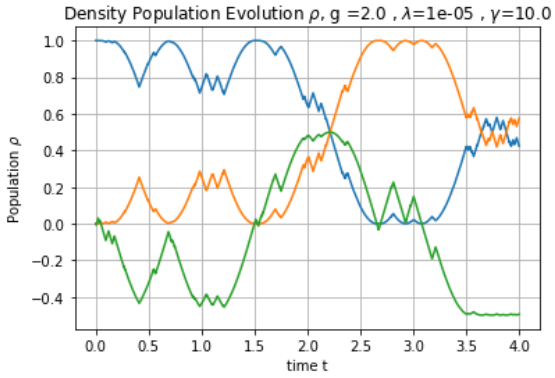

(a) Density Population Evolution

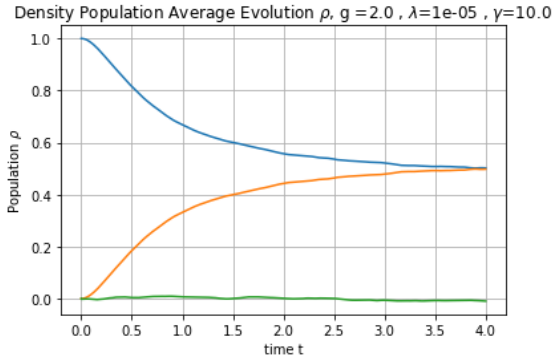

(b) Average Density Population Evolution

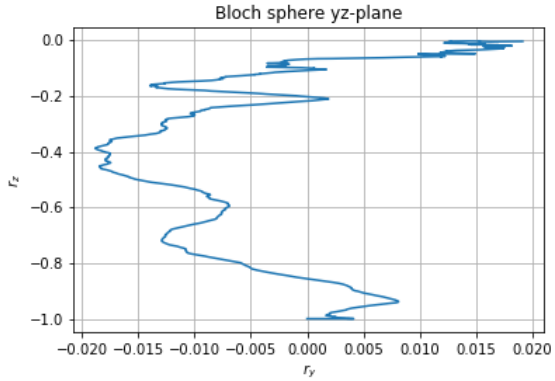

(c) Average Bloch vector $\vec{r}$

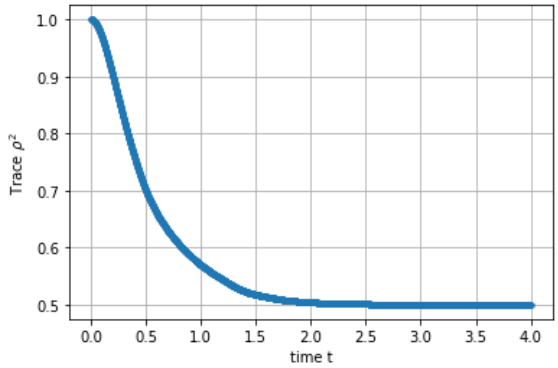

(d) Trace evolution

Figure 4: *Figures* (4a), (4b), (4c), & (4d) including feedback for $\lambda = 1.0 \cdot 10^{-5}$ and $g = 2.0$ for $M = 2500$ trajectories. ρ_{00}, ρ_{11}, α^*. The time t in the plots are in seconds s.

Considering the smallest measurement strength $\lambda = 1.0 \cdot 10^{-5}$, the density evolution plot *Fig.* (4a), for a randomized parameter z, shows that the states vary only slightly and there is no noise. The lack of noise can be explained by the fact that the measurement strength is so small that there is no backaction on the system. The *Fig.* (4b) shows how over time the system will collapse to the mixed states to either the ground state $|0\rangle$ ρ_{00} or the excited state $|1\rangle$ ρ_{11} with equal probability. Since the measurement strength is negligible, the evolution of the states naturally tend to the expected value of $\rho_{00} = 0.5$ and $\rho_{11} = 0.5$. In *Fig.* (4c), one can see that the state vector $\vec{r}$ has a random behaviour, which way be explained by the fact that the measurement strength is too small $\lambda \ll 1$ in order for the feedback function *Eq.*(52) to have any effect, but it eventually tends to the completely *mixed state* $\frac{1}{2}(|0\rangle\langle 0| + |1\rangle\langle 1|)$, supported by the *trace purity plot Fig.* (4d). As expected the *purity* converges $\hat{\rho} \to 0.5$, shown in *Fig.* (4d), indicating that only the *populations* ρ_{00} and ρ_{11} remain. Due to the weak measurement strength in *Eq.*(48), $z(t)$ fluctuates heavily such that the feedback in *Eq.*(50) is applied randomly, resulting in random rotations of the Bloch vector $\vec{r}$. Consequently, the system does not evolve such as the *Rabi oscillator* (c.f. 2.3.2). The random feedback results in a dephase of the system, but it is not evident why this occurs (c.f. *Fig.* (1)).

Measurement Strength $\lambda = 1.0 \cdot 10^{-5}$ and $g = 5.0$

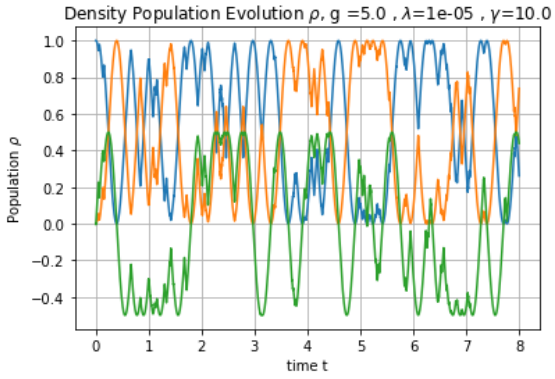

(a) Density Population Evolution

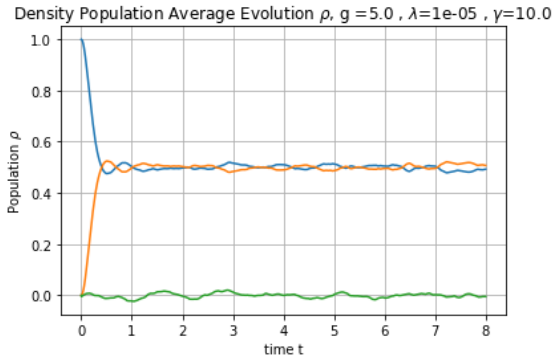

(b) Average Density Population Evolution

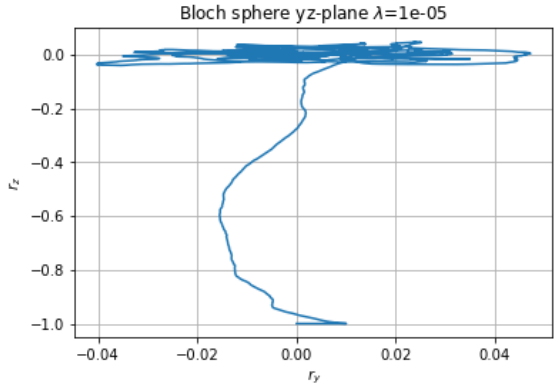

(c) Average Bloch vector $\vec{r}$

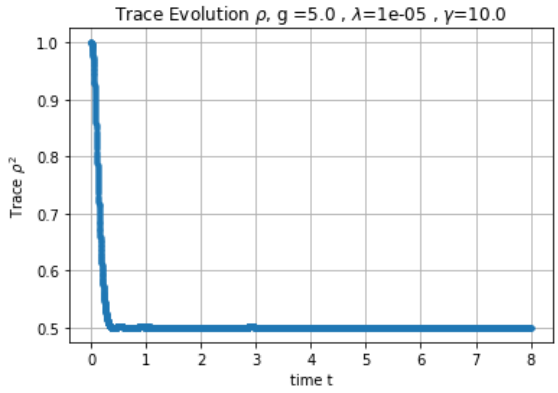

(d) Trace evolution

Figure 5: *Figures* (5a), (5b), (5c), & (5d) including feedback for $\lambda = 1.0 \cdot 10^{-5}$ and $g = 5.0$ for $M = 2500$ trajectories. ρ_{00}, ρ_{11}, α^*. The time t in the plots are in seconds s.

The increase in the interaction strength g to 5.0 leads to a quicker convergence to the completely mixed state $\frac{1}{2}(|0\rangle\langle 0| + |1\rangle\langle 1|)$ as shown in both *Fig.*(5b) and *Fig.*(5d). One may conclude, that the speed of dephasing correlates to the interaction strength g.

Measurement Strength $\lambda = 1.5$ and $g = 2.0$

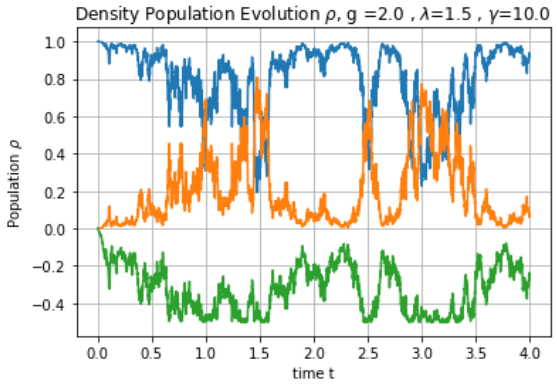

(a) Density Population Evolution

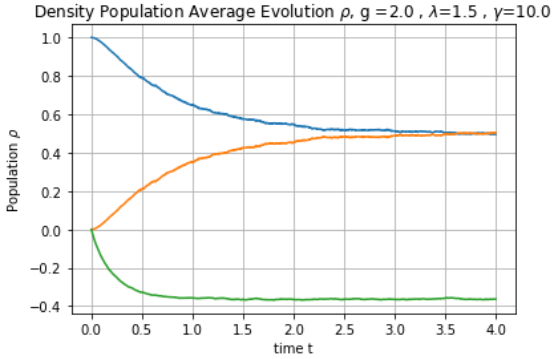

(b) Average Density Population Evolution

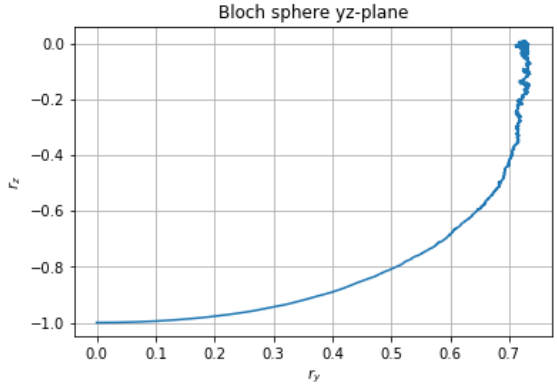

(c) Average Bloch vector $\vec{r}$

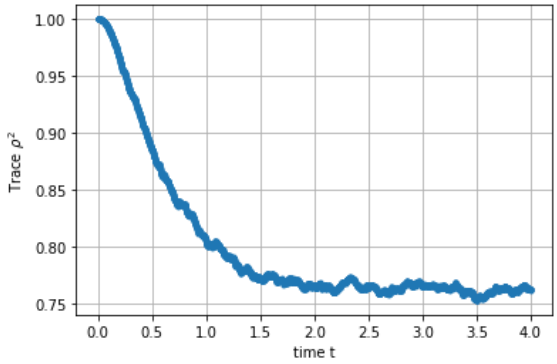

(d) Trace evolution

Figure 6: *Figures* (6a), (6b), (6c), & (6d) including feedback for $\lambda = 1.5$ and $g = 2.0$ for $M = 2500$ trajectories. ρ_{00}, ρ_{11}, α^*. The time t in the plots are in seconds s.

The average density population evolution (c.f. *Fig.* (6b)) converges at a faster rate towards the expectation value $\langle\hat{\rho}\rangle \to 0.5$ than for the smaller measurement strength. As for the Bloch sphere, the Bloch vector $\vec{r}$ points in the direction of the state $\frac{1}{\sqrt{2}}(|0\rangle + i\,|1\rangle)$, but the *purity* does not yield 1, implying that it one is dealing with a mixed state. The *purity* plot (c.f. *Fig.* (6d)) indicates that with a higher measurement strength approaching the interaction strength $\lambda = 1.5 \sim g = 2.0$, the *populations* are attained at a similar time frame than for $\lambda = 1.0 \cdot 10^{-5}$ with more fluctuations. These fluctuations could be explained through the larger backaction between the measurement operator $\hat{K}(z)$ (c.f. *Eq.*(33)) and the system.

Measurement Strength $\lambda = 1.5$ and $g = 5.0$

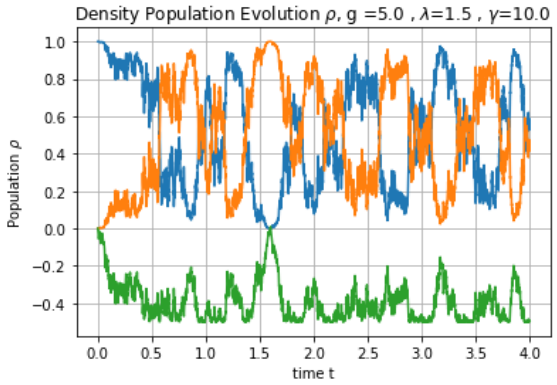

(a) Density Population Evolution

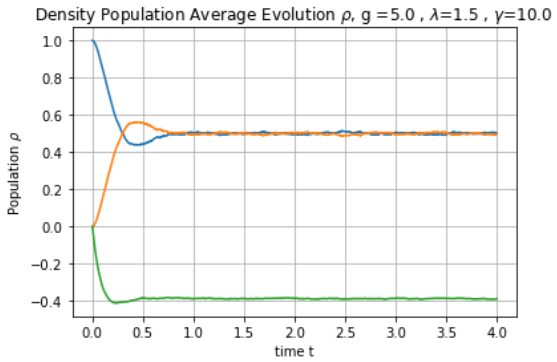

(b) Average Density Population Evolution

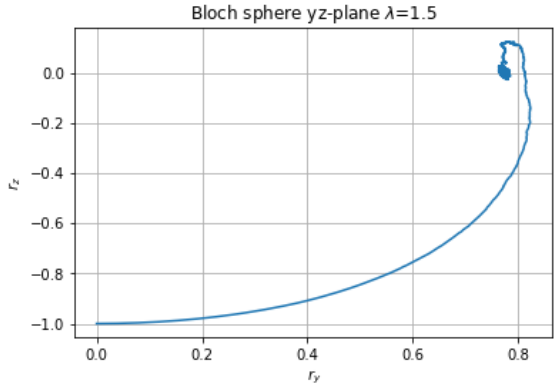

(c) Average Bloch vector $\vec{r}$

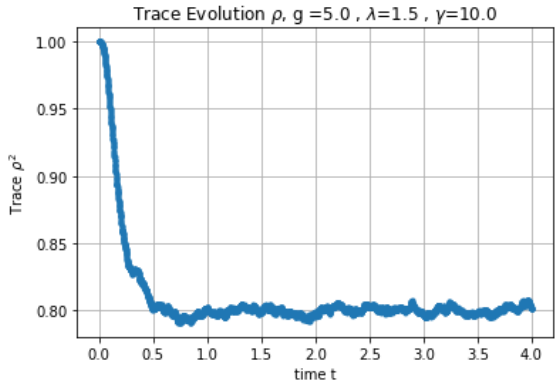

(d) Trace evolution

Figure 7: *Figures* (7a), (7b), (7c), & (7d) including feedback for $\lambda = 1.5$ and $g = 5.0$ for $M = 2500$ trajectories. ρ_{00}, ρ_{11}, α^*. The time t in the plots are in seconds s.

The average density population evolution for $g = 5.0$ results in an increase of the purity, leading to approaching the state $\frac{1}{\sqrt{2}}(|0\rangle + i\,|1\rangle)$.

Measurement Strength $\lambda = 1.5$ and $g = 10.0$

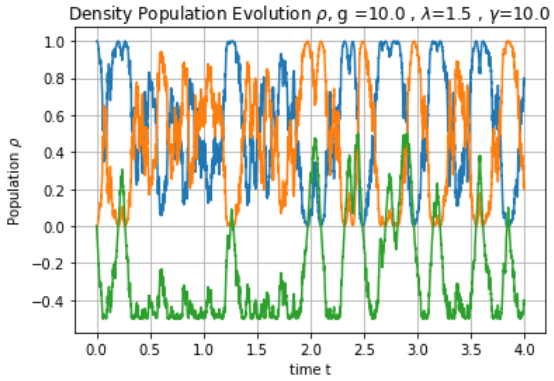

(a) Density Population Evolution

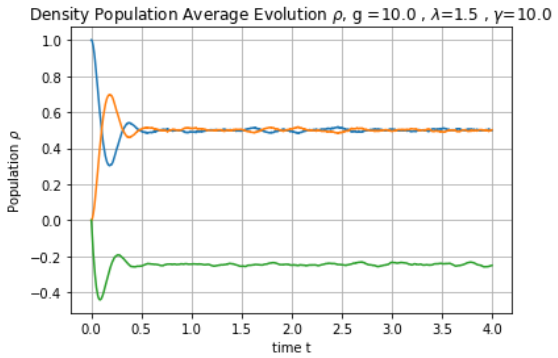

(b) Average Density Population Evolution

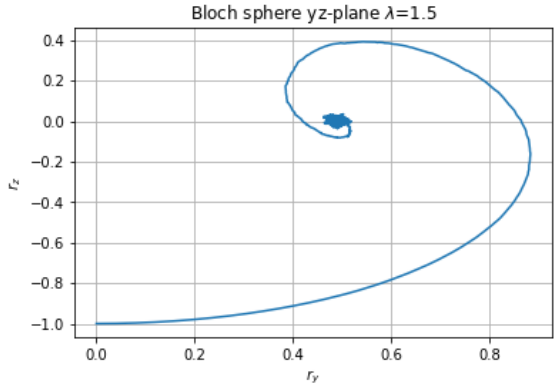

(c) Average Bloch vector $\vec{r}$

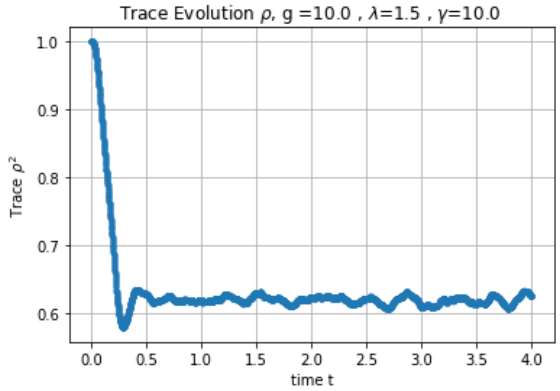

(d) Trace evolution

Figure 8: *Figures* (8a), (8b), (8c), & (8d) including feedback for $\lambda = 1.5$ and $g = 10.0$ for $M = 2500$ trajectories. ρ_{00}, ρ_{11}, α^*. The time t in the plots are in seconds s.

The density population evolution shows much more noise, as shown in *Fig.* (8a). The Bloch sphere plot *Fig.* (8c) shows that the Bloch vector $\vec{r}$ points towards the state $\frac{1}{\sqrt{2}}(|0\rangle + i\,|1\rangle)$. The *Fig.* (8c) shows that the strong interaction energy leads to a strong dephasing, translating to the state vector $\vec{r}$ getting closer to the origin.

Measurement Strength $\lambda = 5.0$ and $g = 2.0$

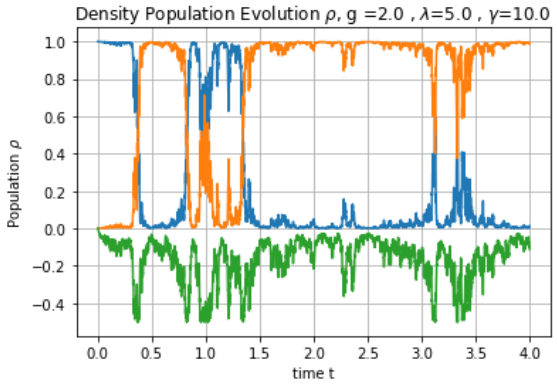

(a) Density Population Evolution

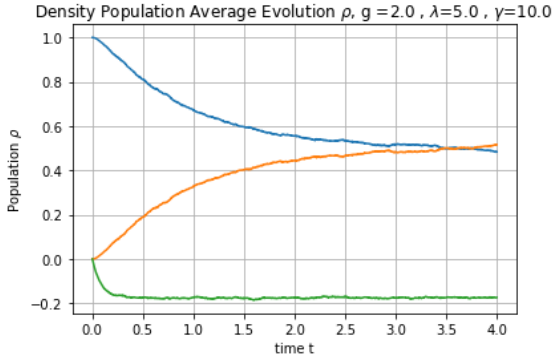

(b) Average Density Population Evolution

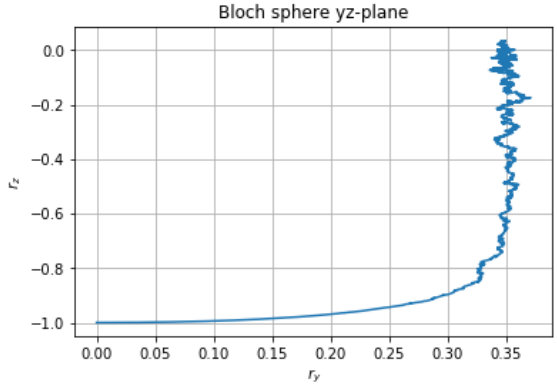

(c) Average Bloch vector $\vec{r}$

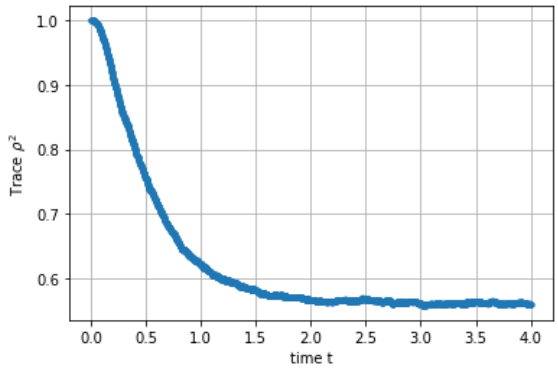

(d) Trace evolution

Figure 9: *Figures* (9a), (9b), (9c), & (9d) including feedback for $\lambda = 5.0$ and $g = 2.0$ for $M = 2500$ trajectories. ρ_{00}, ρ_{11}, α^*. The time t in the plots are in seconds s.

In this particular case, the density population plot has sudden spikes as can be seen in *Fig.* (9a), which is due to the high measurement strength corresponding to a strong interaction with the system. Additionally, the state vector $\vec{r}$ oscillates in the vicinity of $r_y = 0.35$ suggesting that the feedback has a strong backaction impact at the beginning but then loses it's influence over time, resulting in a lower *purity* i.e. approaching even more the origin. The average density population evolution plot *Fig.* (9b) is comparable to that of the plot *Fig.* (6b).

Measurement Strength $\lambda = 5.0$ and $g = 5.0$

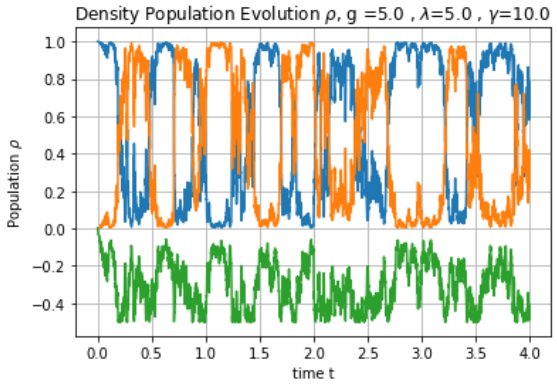

(a) Density Population Evolution

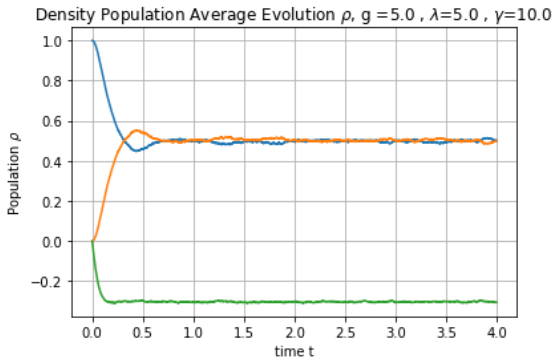

(b) Average Density Population Evolution

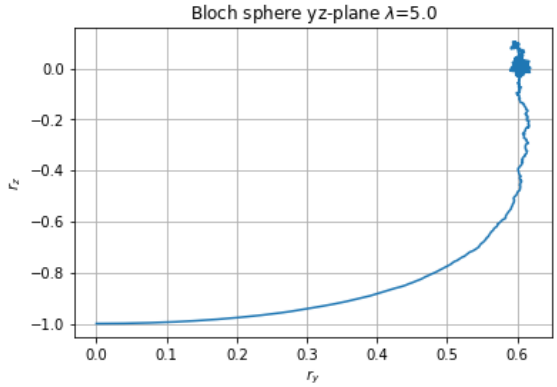

(c) Average Bloch vector $\vec{r}$

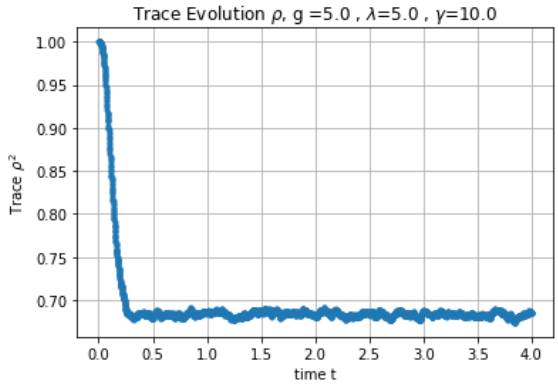

(d) Trace evolution

Figure 10: *Figures* (10a), (10b), (10c), & (10d) including feedback for $\lambda = 5.0$ and $g = 5.0$ for $M = 2500$ trajectories. ρ_{00}, ρ_{11}, α^*. The time t in the plots are in seconds s.

In the case where $\lambda = 5.0$ and $g = 5.0$, the states fluctuate very strongly and one could imply that there is a *steady state coherence*, as can be shown in *Fig.* (10b) as well as *Fig.* (10d). The Bloch sphere plot shows that the state vector $\vec{r}$ points towards the state $\frac{1}{\sqrt{2}}(|0\rangle + i\,|1\rangle)$ and slight oscillations occur towards the end of the simulation. A small interaction strength corresponds to a greater *purity* as indicated in *Fig.* (10c).

Measurement Strength $\lambda = 5.0$ and $g = 10.0$

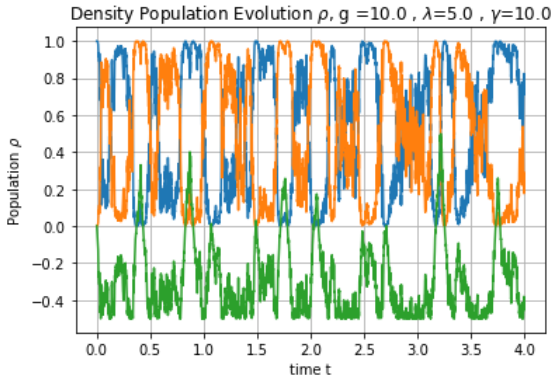

(a) Density Population Evolution

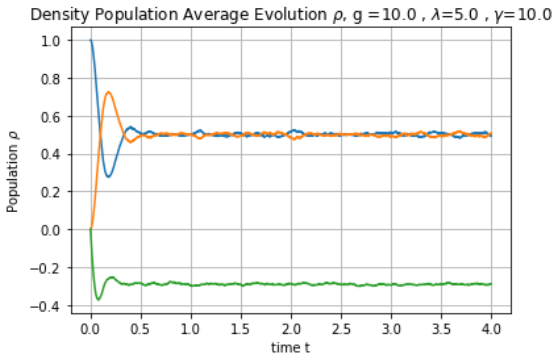

(b) Average Density Population Evolution

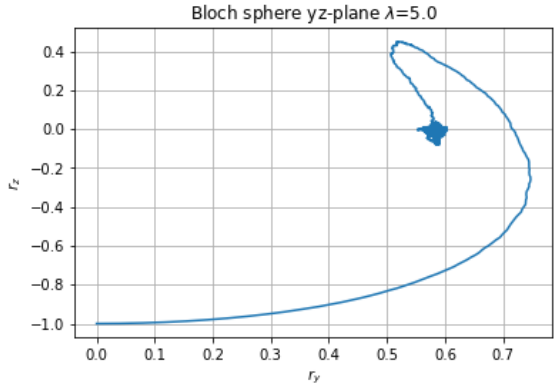

(c) Average Bloch vector $\vec{r}$

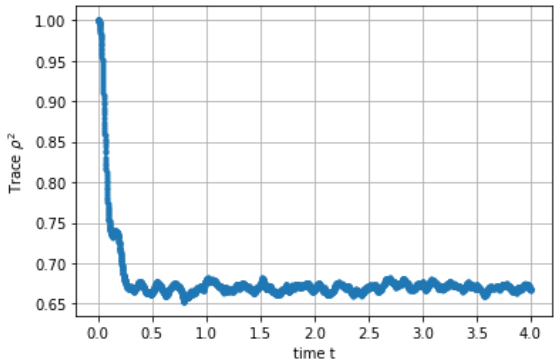

(d) Trace evolution

Figure 11: *Figures* (11a), (11b), (11c), & (11d) including feedback for $\lambda = 5.0$ and $g = 10.0$ for $M = 2500$ trajectories. ρ_{00}, ρ_{11}, α^*. The time t in the plots are in seconds s.

The figures above show what would occur if both the *measurement strength* $\lambda = 5.0$ and the *interaction strength* $g = 10.0$ are high. The most interesting observation is how the state vector $\vec{r}$ moves over time. One can point out that the feedback has a very strong impact and seems to stabilize around the same area as in the other cases (c.f. *Fig.* (11c)). The trace plot shows, *Fig.* (11d), an immediate drop in the *purity*, and hence a *mixed state* is obtained. The previously mentioned dephasing and decrease in *purity* occurs in this case again as shown *Fig.*(11c).

Generally speaking, the Zeno effect seems not to be apparent. The Zeno effect dominates when the off-diagonal terms of the density matrix vanish due to the backaction of the continuous measurement, such that the system cannot evolve any more. The parameters for which the coherence vanishes can be seen in *Fig.* (4b) and *Fig.* (5b). Since the measurement strength is small in both cases, one can possibly trace back the vanishing of the coherences to the random feedback killing off the coherences. However, it is not known to us, why this occurs.

5 Outlook

In this project, one was able to assess how in a two-level system the states evolve over time with feedback control $D(t)$, as well as determine which parameters: measurement strength λ, interaction strength g and the delay factor of the feedback control γ affect the state of the system. The results are best explained with a average density evolution plot, trace evolution plot and Bloch's sphere vector plot. Given the results it is clear that there is an interplay between the measurement strength λ and the interaction strength g, which determines the *purity* of the state. Future endeavours have to determine if it is possible to reach a completely pure state when using feedback in the system. Applications of this project are e.g. quantum error correction [10], atomic clocks [11] and quantum state stabilization [12]. Experiments have been conducted on several applications related to quantum measurements e.g. *Feedback cooling of a one-electron oscillator* [13], *Feedback cooling of a single trapped ion* [14] and *Experimental feedback control of quantum systems using weak measurements* [15] to name a few.

Appendix

5.1 Cyclic Permutation

A crucial property of the *trace*, known as *cyclic permutation*, is the switching of two related operators [5]

$$\begin{aligned} Tr\{\hat{A}\hat{B}\} &= \int \langle x|\hat{A}\hat{B}|x\rangle \, dx \\ &= \int dx \int \langle x|\hat{A}|x'\rangle \, \langle x'|\hat{B}|x\rangle \, dx' \\ &= \int dx' \int \langle x'|\hat{B}|x\rangle \, \langle x|\hat{A}|x'\rangle \, dx' \\ &= \int \langle x'|\hat{B}\hat{A}|x\rangle \, dx' \\ &= Tr\{\hat{B}\hat{A}\}. \end{aligned}$$

Measurement Operator & Property Calculation

$$\begin{aligned} &\mathbb{I} = |0\rangle \langle 0| + |1\rangle \langle 1| , \\ &\hat{z}^\dagger = \hat{z}, \\ &\exp\Big\{\hat{A}\Big\} := \sum_{j=0}^{\infty} \frac{\hat{A}^j}{j!}, \\ &\hat{\sigma}_z |0\rangle = -1 |0\rangle , \\ &\hat{\sigma}_z |1\rangle = 1 |1\rangle , \\ &\mathbb{I}^N = \mathbb{I}. \end{aligned} \tag{54}$$

$$\int_{-\infty}^{\infty}\left(\frac{2\lambda\delta t}{\pi}\right)^{1/2} e^{-\lambda\delta t(\hat{z}-\hat{\sigma}_z)^{2\dagger}}\cdot(|0\rangle\langle 0|+|1\rangle\langle 1|)\cdot e^{-\lambda\delta t(\hat{z}-\hat{\sigma}_z)}\cdot(|0\rangle\langle 0|+|1\rangle\langle 1|)dz=\mathbb{I}$$

$$\iff \left(\frac{2\lambda\delta t}{\pi}\right)^{1/2}\int_{-\infty}^{\infty} e^{-\lambda\delta t(\hat{z}^{\dagger}-\hat{\sigma}_z^{\dagger})^2}\cdot(|0\rangle\langle 0|+|1\rangle\langle 1|)\cdot e^{-\lambda\delta t(\hat{z}-\hat{\sigma}_z)}\cdot(|0\rangle\langle 0|+|1\rangle\langle 1|)dz=\mathbb{I}$$

$$\iff \left(\frac{2\lambda\delta t}{\pi}\right)^{1/2}\int_{-\infty}^{\infty} e^{-\lambda\delta t(\hat{z}-\hat{\sigma}_z)^2}\cdot(|0\rangle\langle 0|+|1\rangle\langle 1|)\cdot e^{-\lambda\delta t(\hat{z}-\hat{\sigma}_z)}\cdot(|0\rangle\langle 0|+|1\rangle\langle 1|)dz=\mathbb{I}$$

$$\iff \left(\frac{2\lambda\delta t}{\pi}\right)^{1/2}\int_{-\infty}^{\infty}\left(e^{-\lambda\delta t(\hat{z}-\hat{\sigma}_z)^2}\cdot(|0\rangle\langle 0|+|1\rangle\langle 1|)\right)^2 dz=\mathbb{I}$$

$$\iff \left(\frac{2\lambda\delta t}{\pi}\right)^{1/2}\int_{-\infty}^{\infty} e^{-2\lambda\delta t(\hat{z}-\hat{\sigma}_z)^2}\cdot(|0\rangle\langle 0|+|1\rangle\langle 1|)dz=\mathbb{I}$$

$$\iff \left(\frac{2\lambda\delta t}{\pi}\right)^{1/2}\cdot\left[\int_{-\infty}^{\infty} e^{-2\lambda\delta t(\hat{z}-\hat{\sigma}_z)^2}\cdot|0\rangle\langle 0|\,dz+\int_{-\infty}^{\infty} e^{-2\lambda\delta t(\hat{z}-\hat{\sigma}_z)^2}\cdot|1\rangle\langle 1|)dz\right]=\mathbb{I}$$

$$\iff \left(\frac{2\lambda\delta t}{\pi}\right)^{1/2}\cdot\left[\sqrt{\frac{\pi}{2\lambda\delta t}}\,|0\rangle\langle 0|+\sqrt{\frac{\pi}{2\lambda\delta t}}\,|1\rangle\langle 1|\right]=\mathbb{I}$$

$$\iff \mathbb{I}=\mathbb{I}\quad\square$$

Density Operator & Measurement Operator Behaviour Calculation

$$\hat{f}(z) = \sqrt{\frac{2\lambda\delta t}{\pi}} \cdot \Bigg[P_0 \cdot e^{-\lambda\delta t(\hat{z}-\hat{\sigma}_z)^2} |0\rangle\langle 0| e^{-\lambda\delta t(\hat{z}-\hat{\sigma}_z)^{2\dagger}} + \alpha e^{-\lambda\delta t(\hat{z}-\hat{\sigma}_z)^2} |0\rangle\langle 1| e^{-\lambda\delta t(\hat{z}-\hat{\sigma}_z)^{2\dagger}}$$

$$+ \alpha e^{-\lambda\delta t(\hat{z}-\hat{\sigma}_z)^2} |1\rangle\langle 0| e^{-\lambda\delta t(\hat{z}-\hat{\sigma}_z)^{2\dagger}} + P_1 e^{-\lambda\delta t(\hat{z}-\hat{\sigma}_z)^2} |1\rangle\langle 1| e^{-\lambda\delta t(\hat{z}-\hat{\sigma}_z)^{2\dagger}} \Bigg]$$

$$\iff \hat{f}(z) = \sqrt{\frac{2\lambda\delta t}{\pi}} \cdot \Bigg[P_0 \cdot e^{-\lambda\delta t(\hat{z}-\hat{\sigma}_z)^2} |0\rangle\langle 0| e^{-\lambda\delta t(\hat{z}-\hat{\sigma}_z)^2} + \alpha e^{-\lambda\delta t(\hat{z}-\hat{\sigma}_z)^2} |0\rangle\langle 1| e^{-\lambda\delta t(\hat{z}-\hat{\sigma}_z)^2}$$

$$+ \alpha e^{-\lambda\delta t(\hat{z}-\hat{\sigma}_z)^2} |1\rangle\langle 0| e^{-\lambda\delta t(\hat{z}-\hat{\sigma}_z)^2} + P_1 e^{-\lambda\delta t(\hat{z}-\hat{\sigma}_z)^2} |1\rangle\langle 1| e^{-\lambda\delta t(\hat{z}-\hat{\sigma}_z)^2} \Bigg]$$

$$\iff \hat{f}(z) = \sqrt{\frac{2\lambda\delta t}{\pi}} \cdot \Bigg[P_0 \cdot e^{-\lambda\delta t(\hat{z}+1)^2} |0\rangle\langle 0| e^{-\lambda\delta t(\hat{z}+1)^2} + \alpha e^{-\lambda\delta t(\hat{z}+1)^2} |0\rangle\langle 1| e^{-\lambda\delta t(\hat{z}-1)^2}$$

$$+ \alpha e^{-\lambda\delta t(\hat{z}-1)^2} |1\rangle\langle 0| e^{-\lambda\delta t(\hat{z}+1)^2} + P_1 e^{-\lambda\delta t(\hat{z}-1)^2} |1\rangle\langle 1| e^{-\lambda\delta t(\hat{z}-1)^2} \Bigg]$$

$$\iff \hat{f}(z) = \sqrt{\frac{2\lambda\delta t}{\pi}} \cdot \Bigg[P_0 \cdot e^{-2\lambda\delta t(\hat{z}+1)^2} |0\rangle\langle 0| + \alpha e^{-2\lambda\delta t(\hat{z}^2+1)} |0\rangle\langle 1|$$

$$+ \alpha e^{-2\lambda\delta t(\hat{z}^2+1)} |1\rangle\langle 0| + P_1 e^{-2\lambda\delta t(\hat{z}-1)^2} |1\rangle\langle 1| \Bigg]$$

$$\lambda \to \infty \implies \hat{f}(z) = \sqrt{\frac{2\lambda\delta t}{\pi}} \cdot \Bigg[P_0 \cdot e^{-2\lambda\delta t(\hat{z}+1)^2} |0\rangle\langle 0| + P_1 e^{-2\lambda\delta t(\hat{z}-1)^2} |1\rangle\langle 1| \Bigg]$$

$$\lambda \to 0 \implies \hat{f}(z) = 0$$

$$\begin{aligned}
\int_{-\infty}^{\infty} \hat{f}(z)dz &= \sqrt{\frac{2\lambda\delta t}{\pi}} \cdot \int_{-\infty}^{\infty} \Bigg[P_0 \cdot e^{-2\lambda\delta t(\hat{z}+1)^2} |0\rangle\langle 0| + P_1 e^{-2\lambda\delta t(\hat{z}-1)^2} |1\rangle\langle 1| \Bigg] dz, \\
&= \sqrt{\frac{2\lambda\delta t}{\pi}} \cdot \Bigg[P_0 \int_{-\infty}^{\infty} e^{-2\lambda\delta t(\hat{z}+1)^2} |0\rangle\langle 0| \, dz + P_1 \int_{-\infty}^{\infty} e^{-2\lambda\delta t(\hat{z}-1)^2} |1\rangle\langle 1| \, dz \Bigg], \\
&= \sqrt{\frac{2\lambda\delta t}{\pi}} \cdot \Bigg[P_0 \cdot \sqrt{\frac{\pi}{2\lambda\delta t}} \delta(z+1) |0\rangle\langle 0| + P_1 \cdot \sqrt{\frac{\pi}{2\lambda\delta t}} \delta(z-1) |1\rangle\langle 1| \Bigg], \\
&= P_0 \cdot \delta(z+1) |0\rangle\langle 0| + P_1 \cdot \delta(z-1) |1\rangle\langle 1|
\end{aligned}$$

Rabi Oscillator Calculation

Time-Dependent Two-State Problem

As described in *Sakurai* [6], one may construct the *time-dependent two-state* problem as follows

$$\begin{aligned}
&\hat{H} = E_1 \left|\alpha_1\right\rangle \left\langle\alpha_1\right| + E_2 \left|\alpha_2\right\rangle \left\langle\alpha_2\right|, \ E_1 < E_2, \\
&V(t) = \gamma e^{i\omega t} \left|\alpha_1\right\rangle \left\langle\alpha_2\right| + \gamma e^{-i\omega t} \left|\alpha_2\right\rangle \left\langle\alpha_1\right|, \\
&\omega_{12} = \frac{E_2 - E_1}{\hbar}
\end{aligned}$$

The probabilities of the problem are given as follows

$$\begin{aligned}
&|c_1(t)|^2 + |c_2(t)|^2 = 1, \\
&|c_2(t)|^2 = \frac{\gamma^2/\hbar^2}{\gamma^2/\hbar^2 + (\omega - \omega_{12})^2/4} \cdot \sin\left\{\sqrt{\left[\frac{\gamma^2}{\hbar^2} + \frac{(\omega - \omega_{12})^2}{4}\right]} t\right\}, \\
&|c_1(t)|^2 = 1 - |c_2(t)|^2
\end{aligned}$$

$$\begin{aligned}
\frac{d\hat{\rho}}{dt} &= -i \cdot \left[g\Big(\left|0\right\rangle \left\langle 1\right| + \left|1\right\rangle \left\langle 0\right| \Big), \hat{\rho} \right] + 0 \\
&= -i \cdot \Bigg[g\Big(\left|0\right\rangle \left\langle 1\right| + \left|1\right\rangle \left\langle 0\right| \Big) \cdot \Big(P_0(t) \left|0\right\rangle \left\langle 0\right| + \alpha(t) \left|0\right\rangle \left\langle 1\right| + \alpha^*(t) \left|1\right\rangle \left\langle 0\right| + P_1(t) \left|1\right\rangle \left\langle 1\right| \Big) \\
&- \Big(P_0(t) \left|0\right\rangle \left\langle 0\right| + \alpha(t) \left|0\right\rangle \left\langle 1\right| + \alpha^*(t) \left|1\right\rangle \left\langle 0\right| + P_1(t) \left|1\right\rangle \left\langle 1\right| \Big) \cdot g\Big(\left|0\right\rangle \left\langle 1\right| + \left|1\right\rangle \left\langle 0\right| \Big) \Bigg] \\
&= -i \cdot \Big[\Big(P_1(t)g \left|0\right\rangle \left\langle 1\right| + \alpha^*(t)g \left|0\right\rangle \left\langle 0\right| + P_0(t)g \left|1\right\rangle \left\langle 0\right| + \alpha(t) \left|1\right\rangle \left\langle 1\right| \Big) \\
&- \Big(P_0(t)g \left|0\right\rangle \left\langle 1\right| + \alpha^*(t)g \left|1\right\rangle \left\langle 1\right| + \alpha(t)g \left|0\right\rangle \left\langle 0\right| + P_1(t)g \left|1\right\rangle \left\langle 0\right| \Big) \Big] \\
&= -i \cdot \Big[\Big(P_1(t)g - P_0(t)g \Big) \cdot \left|0\right\rangle \left\langle 1\right| + \Big(\alpha^*(t)g - \alpha(t)g \Big) \cdot \left|0\right\rangle \left\langle 0\right| \\
&+ \Big(P_0(t)g - P_1(t)g \Big) \cdot \left|1\right\rangle \left\langle 0\right| + \Big(\alpha(t)g - \alpha^*(t)g \Big) \cdot \left|1\right\rangle \left\langle 1\right| \Big]
\end{aligned}$$

References

[1] Dantas, A. D., Dantas, A. F., Campos, J. T., de Almeida Neto, D. L., and Dórea, C. E. (2018). PID control for electric vehicles subject to control and speed signal constraints. Journal of Control Science and Engineering, 2018, 1–11. https://doi.org/10.1155/2018/6259049

[2] Wikimedia Foundation, Inc. (2022, February 23). Monte Carlo Method. Wikipedia. Retrieved March 8, 2022, from https://en.wikipedia.org/wiki/Monte_Carlo_method

[3] Nielsen, M. A., and Chuang, I. L. (2021). Quantum Computation and Quantum Information. Cambridge University Press.

[4] Wikimedia Foundation, Inc. (2022, May 12). Qubit. Wikipedia. Retrieved June 7, 2022, from https://en.wikipedia.org/wiki/Qubit

[5] Jacobs, K., and Steck, D. A. (2007, February 20). Contemporary Physics: A straightforward introduction to continuous quantum measurement. London; Taylor &; Francis Group.

[6] Sakurai, J. J., and Napolitano, J. (2021). Modern Quantum Mechanics (3rd ed.). Cambridge University Press.

[7] Breuer, H.-P., and Petruccione, F. (2010). The Theory of Open Quantum Systems (1st ed.). Oxford University Press.

[8] Itano, W. M., Heinzen, D. J., Bollinger, J. J., and Wineland, D. J. (1990). Quantum Zeno Effect. Physical Review A, 41(5). https://doi.org/https://doi.org/10.1103/PhysRevA.41.2295

[9] Bednorz, A., Belzig, W., and Nitzan, A. (2012, January 6). Nonclassical time correlation functions in continuous quantum measurement. New Journal of Physics. Retrieved May 6, 2022, from https://iopscience.iop.org/article/10.1088/1367-2630/14/1/013009/meta

[10] Sarovar, M., Ahn, C., Jacobs, K., and Milburn, G. J. (2004, May 19). Practical scheme for error control using feedback. Physical Review A. Retrieved May 11, 2022, from https://journals.aps.org/pra/abstract/10.1103/PhysRevA.69.052324

[11] Ludlow, A. D., Boyd, M. M., Ye, J., Peik, E., and Schmidt, P. O. (2015, June 26). Optical atomic clocks. Reviews of Modern Physics. Retrieved May 11, 2022, from https://journals.aps.org/rmp/abstract/10.1103/RevModPhys.87.637

[12] Annby-Andersson, B., Bakhshinezhad, F., Bhattacharyya, D., De Sousa, G., Jarzynski, C., Samuelsson, P., and Potts, P. P. (2021, October 18). Quantum Fokker-Planck master equation for continuous feedback control. arXiv.org. Retrieved May 10, 2022, from https://arxiv.org/abs/2110.09159

[13] D'Urso, B., Odom, B., and Gabrielse, G. (2003, January 28). Feedback cooling of a one-electron oscillator. Physical Review Letters. Retrieved June 8, 2022, from https://journals.aps.org/prl/abstract/10.1103/PhysRevLett.90.043001

[14] Bushev, P., Rotter, D., Wilson, A., Dubin, F., Becher, C., Eschner, J., Blatt, R., Steixner, V., Rabl, P., and Zoller, P. (2006, February 3). Feedback cooling of a single trapped ion. Physical Review Letters. Retrieved June 8, 2022, from https://journals.aps.org/prl/abstract/10.1103/PhysRevLett.96.043003

[15] Gillett, G. G., Dalton, R. B., Lanyon, B. P., Almeida, M. P., Barbieri, M., Pryde, G. J., O'Brien, J. L., Resch, K. J., Bartlett, S. D., and White, A. G. (2010, February 26). Experimental feedback control of quantum systems using weak measurements. Physical Review Letters. Retrieved June 8, 2022, from https://journals.aps.org/prl/abstract/10.1103/PhysRevLett.104.080503